Hydrology and
Earth System
Sciences

Evaluation of precipitation measurement methods using data from a precision lysimeter network

Tobias Schnepper[1,2,3], **Jannis Groh**[1,4,5], **Horst H. Gerke**[4], **Barbara Reichert**[2], and **Thomas Pütz**[1]

[1]Institute of Bio- and Geoscience IBG-3: Agrosphere, Forschungszentrum Jülich GmbH, 52428 Jülich, Germany
[2]Institute for Geosciences, University of Bonn, Nussallee 8, 53113 Bonn, Germany
[3]GFZ German Research Centre for Geosciences, Telegrafenberg, 14473 Potsdam, Germany
[4]Research Area 1 "Landscape Functioning", Leibniz Centre for Agricultural Landscape Research (ZALF),
Eberswalder Straße 84, 15374 Müncheberg, Germany
[5]Institute of Crop Science and Resource Conservation – Soil Science and Soil Ecology,
University of Bonn, Nussallee 13, 53113 Bonn, Germany

Correspondence: Tobias Schnepper (tobias.schnepper@gfz-potsdam.de)

Abstract. Accurate precipitation data are essential for assessing the water balance of ecosystems. Methods for point precipitation determination are influenced by wind, precipitation type and intensity and/or technical issues. High-precision weighable lysimeters provide precipitation measurements at ground level that are less affected by wind disturbances and are assumed to be relatively close to actual precipitation. The problem in previous studies was that the biases in precipitation data introduced by different precipitation measurement methods were not comprehensively compared with and quantified on the basis of those obtained by lysimeters in different regions in Germany.

The aim was to quantify measurement errors in standard precipitation gauges as compared to the lysimeter reference and to analyze the effect of precipitation correction algorithms on the gauge data quality. Both correction methods rely on empirical constants to account for known external influences on the measurements, following a generic and a site-specific approach. Reference precipitation data were obtained from high-precision weighable lysimeters of the TERrestrial ENvironmental Observatories (TERENO)-SOILCan lysimeter network. Gauge types included tipping bucket gauges (TBs), weighable gauges (WGs), acoustic sensors (ASs) and optical laser disdrometers (LDs). From 2015-2018, data were collected at three locations in Germany, and 1 h aggregated values for precipitation above a threshold of 0.1 mm h^{-1} were compared.

The results show that all investigated measurement methods underestimated the precipitation amounts relative to the lysimeter references for long-term precipitation totals with catch ratios (CRs) of between 33 %–92 %. Data from ASs had overall biases of −0.25 to −0.07 mm h^{-1}, while data from WGs and LDs showed the lowest measurement bias (−0.14 to −0.06 mm h^{-1} and −0.01 to −0.02 mm h^{-1}). Two TBs showed systematic deviations with biases of −0.69 to −0.61 mm h^{-1}, while other TBs were in the previously reported range with biases of −0.2 mm h^{-1}. The site-specific and generic correction schemes reduced the hourly measurement bias by 0.13 and 0.08 mm h^{-1} for the TBs and by 0.09 and 0.07 mm h^{-1} for the WGs and increased long-term CRs by 14 % and 9 % and by 10 % and 11 %, respectively.

It could be shown that the lysimeter reference operated with minor uncertainties in long-term measurements under different site and weather conditions. The results indicate that considerable precipitation measurement errors can occur even at well-maintained and professionally operated stations equipped with standard precipitation gauges. This generally leads to an underestimation of the actual precipitation amounts. The results suggest that the application of relatively simple correction schemes, manual or automated data quality checks, instrument calibrations, and/or an adequate choice of observation period can help improve the data quality of gauge-based measurements for water balance calculations, ecosystem modeling, water management, assessment of agri-

cultural irrigation needs, or radar-based precipitation analyses.

1 Introduction

Exact precipitation data are essential to determine the ecosystem water balance within the soil–plant–atmosphere continuum (Porporato and Rodriguez-Iturbe, 2002). To obtain information on local precipitation amounts, point precipitation measurements are carried out using catching and non-catching precipitation gauges (WMO, 2018). At regional and global scales, precipitation measurement networks connecting a variety of rain gauges provide data to calibrate radar precipitation estimates, climate models, and hydrological cycles (Michaelides et al., 2009; Tapiador et al., 2017). Therefore, point precipitation measurements have been intensively studied and several methods for determining precipitation have been developed (WMO, 2018). Depending on the design and functionality of the measuring devices, different errors were identified that affect the precipitation measurements (e.g., Fuchs et al., 2001; Sevruk, 1987; Sevruk and Chvíla, 2005) and therefore also hydrological models (Bárdossy et al., 2022). The influence of wind, in particular, has been shown to negatively affect point precipitation measurements (Chvíla et al., 2005; Duchon and Essenberg, 2001; Pollock et al., 2018; Sevruk et al., 1989). The effect depends on wind speed, shielding, the shape of the precipitation gauge, and the size, phase, and fall velocity of the hydrometeors (Kochendorfer et al., 2017b; Sevruk and Nespor, 1994; Wolff et al., 2015). The use of wind shields (Alter, 1937; Nipher, 1878) can reduce the measurement bias, depending on the shields' design (Kochendorfer et al., 2017a; Watson et al., 2008; Yang et al., 1999a). In order to quantify erroneous point precipitation measurements and to minimize the influence of wind, ground-level gauges were developed (Goodison et al., 1998; Lanza and Vuerich, 2009; Sevruk and Hamon, 1984). The data obtained from these gauges were used as a reference for comprehensive comparisons of precipitation gauges for solid (Goodison et al., 1998) and liquid precipitation (Lanza and Vuerich, 2009). The comparative studies led to the development of correction methods that are applied during the post-processing of the data (Førland et al., 1996; Richter, 1995; Sevruk, 1982).

Weighable lysimeters were recognized in the 1960s as a reference system for precipitation gauge comparisons with measurements at the soil surface (McGuiness, 1966; Morgan and Lourence, 1969). Lysimeters were originally developed to determine and quantify soil- and plant-related processes such as drainage, evapotranspiration, ion exchange, root development, and solute transport (Goss and Ehlers, 2009; Hertel and von Unold, 2013). A direct determination of precipitation with weighable lysimeters has been limited in the past by relatively coarse temporal resolution (> 10 min to daily)

and precision. Within the TERrestrial ENvironmental Observatories (TERENO)-SOILCan lysimeter network, high-precision weighable lysimeters are used that operate with a high temporal resolution (< 1 min; Pütz et al., 2016). These lysimeters have been successfully used for monitoring precipitation, dew, and hoar frost for soil ecosystems (Gebler et al., 2015; Groh et al., 2018b; Schrader et al., 2013) with a greater resolution and precision than most common gauges (Xiao et al., 2009b).

To assure data quality and the reliable accuracy of lysimeter-derived precipitation measurements, Marek et al. (2014) stated that the pre- and post-processing of lysimeter data were highly important. Time series of lysimeter mass changes are oscillating and temporally autocorrelated (Herbrich and Gerke, 2016). Noise-filtering algorithms have therefore been developed since the 2010s to reduce the influence of ambient noise on the data (Hannes et al., 2015; Nolz et al., 2013; Peters et al., 2014; Ross et al., 2020; Vaughan and Ayars, 2009). The "adaptive window and threshold filter" (AWAT; Peters et al., 2014) executes two steps to process the data towards a correction of time-variable noise levels (Peters et al., 2016, 2017). This filter solved the problem of underestimating the lysimeter mass change signals at the turning point from precipitation to evapotranspiration or vice versa; it yields an almost unbiased representation of the real signal, which is especially important for the quantification of smaller flux rates such as those caused, for instance, by dew formation (Groh et al., 2018b; Xiao et al., 2009a).

The increased lysimeter data quality (i.e., precision and temporal resolution) has already led to a number of studies that compared lysimeter measurements with those of other precipitation gauges (Gebler et al., 2015; Haselow et al., 2019; Hoffmann et al., 2016; Kohfahl and Saaltink, 2020; Schrader et al., 2013). Gebler et al. (2015) found a 16 % underestimation of tipping bucket gauge (TB) measured precipitation totals compared to lysimeter data for 1 year, with 17 % of the difference due to rime and dew and 5.5 % due to fog and drizzle. Snow formation also contributed to the deviations, although the authors identified problems with snow bridges and snow drift interfering with the lysimeter measurements (Gebler et al., 2015). Haselow et al. (2019) compared precipitation measured with a piezoelectric precipitation sensor, a standard TB, and a weighable lysimeter. They found an underestimation by the TB and an overestimation by the piezoelectric sensor compared to the lysimeter measurements. Kohfahl and Saaltink (2020) compared precipitation measurements of a precision lysimeter with two TBs and one weighable rain gauge. The authors found good agreement between the measured data from one TB rain gauge, the weighable rain gauge, and the lysimeter, while recommending correction of the data from the other TB, which underestimates precipitation intensities compared to the lysimeter reference.

Within the framework of the TERENO-SOILCan lysimeter network, numerous point precipitation measurement

gauges are in operation, producing data with 10 min resolution (Pütz et al., 2016). Up to four different rain gauges are installed in the immediate vicinity of the lysimeter stations, and their data can be publicly accessed through the TERENO data platform (https://ddp.tereno.net/ddp/, last access: 15 August 2022; for details see the "Data availability" section; Kunkel et al., 2013). The lysimeter data available within the network are comprehensively processed and tested and have been used for a variety of studies in the field of soil and plant sciences (Groh et al., 2019, 2020a).

For this study, we hypothesize that values derived from hourly precipitation data of high-precision weighable lysimeters can function as a reference for a comparison of multiple precipitation measurement methods. To test this, data from multiple lysimeters installed at respective test sites are graphically compared via scatterplots, a correlation coefficient, and deviations from the arithmetic mean. Furthermore, we hypothesize that if the precipitation measurements of the considered methods are affected by external influences, then the gauge measurements should be, on average, lower than the ones determined by the lysimeter references for all devices of the same gauge model at all sites. To test this, we compare hourly precipitation amounts as well as long-term precipitation totals determined by these measurement methods with reference data derived from high-precision weighable lysimeter data via scatterplots and appropriate statistics for all three sites, also considering measurement uncertainties. The final hypothesis is that the use of precipitation correction methods that consider the influence of wind and other typical sources of error on the instruments will reduce the bias between reference and measurements and increase the data quality close to zero. Therefore, two correction methods are applied to the TB and weighable gauge (WG) data during post-processing, and the influence on the bias and overall deviations from the references is studied by comparing the resulting data with the reference lysimeter-based precipitation.

To conduct this study, high-quality long-term data of 4 years (2015–2018) from 15 lysimeters, four different types of precipitation measurement methods (11 devices) for three research sites, and local weather data with a resolution of 1 h are available.

2 Material and methods

2.1 Research sites

The data were collected at research sites near Dedelow (DD), Rollesbroich (RO), and Selhausen (SE) in Germany, which are all part of the TERENO-SOILCan network (Fig. 1; Pütz et al., 2016). The TERENO-SOILCan lysimeter network itself belongs to the TERENO project (Zacharias et al., 2011) and comprises 12 different lysimeter research sites in Germany (Pütz et al., 2016). The network purpose is to enable in-

sights into the effects of climate change on arable and grassland ecosystems, including water balance components. To achieve this, a modified space-for-time concept was used, where lysimeters filled with four different soils were transferred within the TERENO observatories to simulate a time-induced change in climate through a space-induced change in climate to study the effects on crop productivity and soil water and plant nutrient balances (Groh et al., 2020a, b; Pütz et al., 2016). The lysimeters have been used to estimate precipitation and actual evapotranspiration (Gebler et al., 2015; Groh et al., 2019; Schrader et al., 2013) as well as non-rainfall water that arises from the formation of dew, hoar frost, and rime (Groh et al., 2018b; Meissner et al., 2007).

RO, as part of the Eifel/Lower Rhine Valley Observatory, is situated in the northern part of the Eifel, which is a low mountain range in western Germany (Bogena et al., 2018). The area is mostly open, comprises extensively used grassland, and is located 511 m a.s.l. (above sea level). The site in SE is situated in the plain of the lower Rhine Valley and is surrounded by extensively used arable land (Bogena et al., 2018). The test site near DD is in the Northeastern German Lowland Observatory of TERENO (Heinrich et al., 2018), approximately 100 km north of the city of Berlin. At the site, a hummocky ground moraine landscape is characterized by lakes and arable land (Heinrich et al., 2018). More information on the sites is provided in Table 1.

2.2 Equipment and data collection

2.2.1 TERENO-SOILCan lysimeter

The weighable high-precision lysimeters used within the TERENO-SOILCan network are comparable to the "Scientific Field Lysimeter" described by von Unold and Fank (2008). The lysimeters are equipped with soil moisture probes, soil water sampling devices, tensiometer, a precision weighable system, a thermal flux sensor, and silicon carbide porous suction cups (Pütz et al., 2016). Every lysimeter has a surface of $1 \, m^2$ and a depth of 1.5 m. They are connected to a central service well which contains the power supply, data loggers, measuring transducers, pumps, seepage water tanks including weighable systems, sampling bottles, and a data modem (Pütz et al., 2016). For detailed information about the installed sensors and the lysimeter filling, see Pütz et al. (2016) and Hertel and von Unold (2013).

All lysimeters used in this study are of the same type and arranged in lysimeter stations which comprise at least one hexagon of six lysimeters placed around the central service well (Fig. 2a; Pütz et al., 2016). The hexagon area covers approximately $49 \, m^2$ in total (Fig. 2a). The precipitation gauges and weather stations are located directly adjacent (Fig. 2b), except for one tipping bucket gauge in Rollesbroich, which is located around 30 m from the respective lysimeter hexagon.
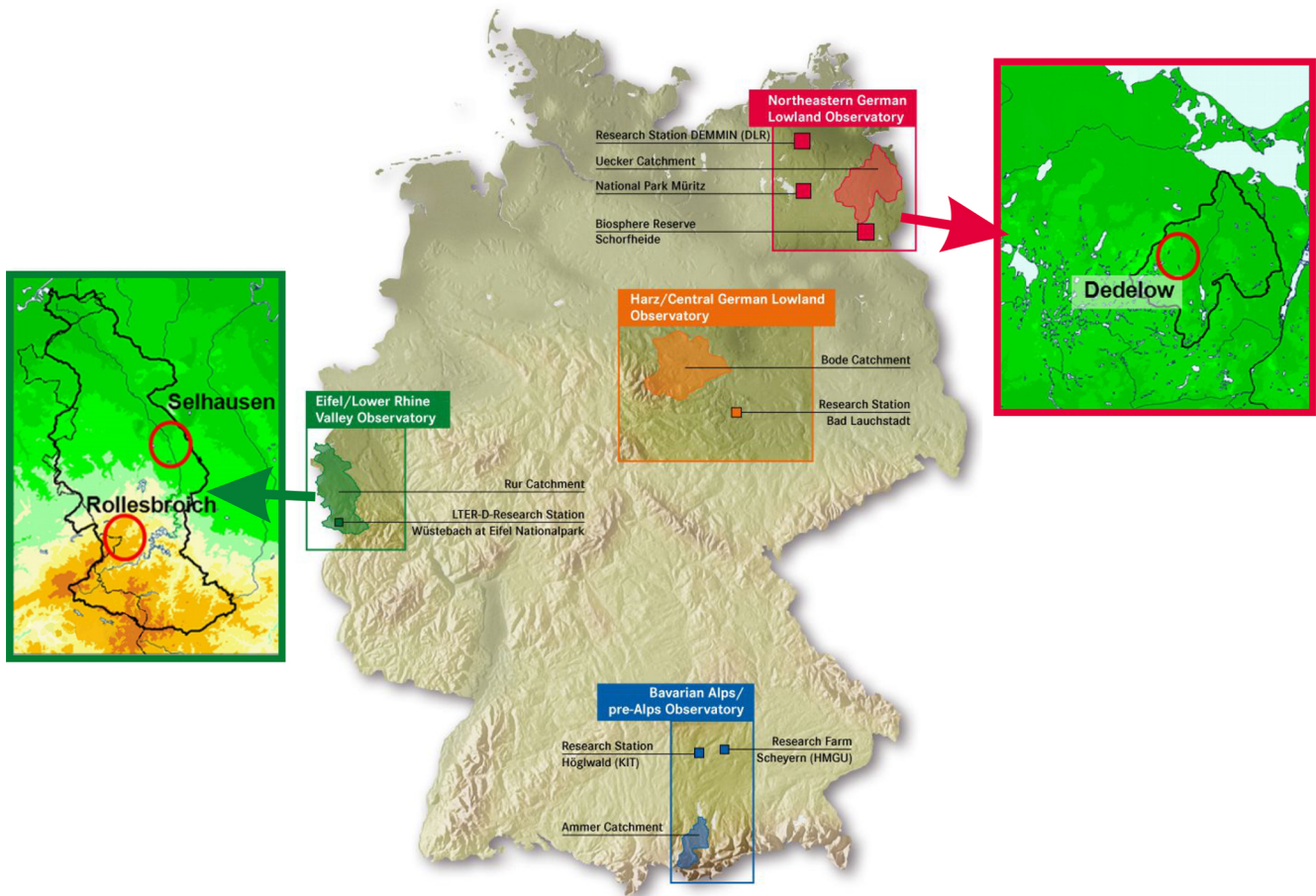
Figure 1. The TERrestrial ENvironmental Observatories (TERENO)-SOILCan network (adapted from Pütz et al., 2016). The data for this study were collected at sites near Dedelow (Northeastern German Lowland Observatory), Rollesbroich, and Selhausen (both Eifel/Lower Rhine Valley Observatory).

Table 1. Information on site characteristics, annual mean precipitation (DWD, 2021a) and annual mean temperature (DWD, 2021b) based on multi-year averages (1961–1999).

	Mean annual precipitation (mm)	Mean annual temperature (°C)	Coordinates (° N, ° E)	Dominant land use (–)
Rollesbroich	1063	7.7	50°37′, 06°18′	Grassland
Selhausen	723	9.8	50°52′, 06°27′	Arable land
Dedelow	504	7.9	53°22′, 13°48′	Arable land

The weighable systems within the lysimeter consist of three load cells (Model 3510, Tedea-Huntleigh, Canoga Parl, CA, USA) with a resolution of $10 \, \text{g} \cong 0.01$ mm precipitation and are mounted at each lysimeters bottom. A gap between lysimeter and the concrete housing is closed with a synthetic resin collar, which is covered with surrounding soil. The small remaining gap between the collar and the lysimeter is closed with silicone foil fixed at the resin collar but without any direct contact to the lysimeter vessel to prevent any disturbance on the lysimeter weighing. This ensures a smooth suspension and weighing of the lysimeter (Pütz et al., 2016). The lysimeters were intensively maintained at least every week and the incoming data were checked daily for irregularities and anomalies. To ensure a stable environment for the observations, the type of lysimeter filling remains the same during the observation period. The surrounding areas were managed similarly to the lysimeters to prevent an "island effect" that would have affected the determination
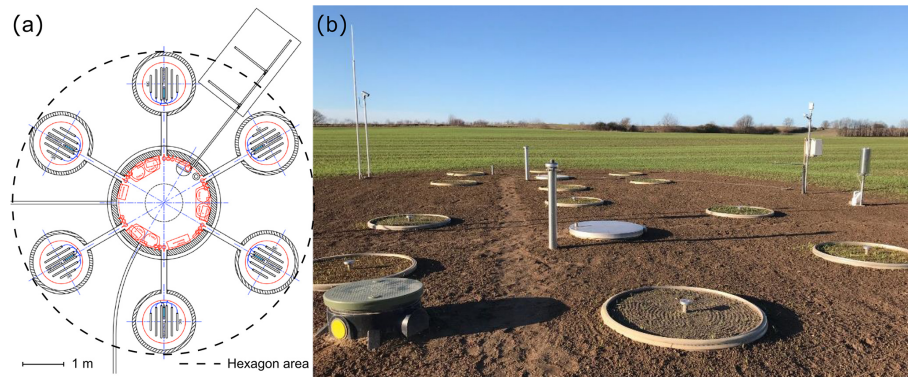
Figure 2. (a) Bird's-eye view technical drawing of the lysimeter hexagon (from Pütz et al., 2016, provided by UMS AG, Munich, Germany). Six lysimeters with surface areas of 1 m² each are located equidistant from the central service well. **(b)** Two lysimeter hexagons at ZALF's research station in Dedelow. Tipping bucket and acoustic sensor are installed directly adjacent to the lysimeter (photo by Hannah Kimmich).

of precipitation due to exposed vegetation (Hagenau et al., 2015). On the arable lysimeters the crop rotation was winter wheat, winter barley, winter rye, and oat during the observation period (2015–2018). No catch crop between the growing seasons was grown. In general, the agricultural activities were in accordance with common agricultural practice (Pütz et al., 2016). The grass lysimeters were cut three to four times per year.

Based on the mass changes in a lysimeter and a seepage water tank, the water fluxes across the soil surface were calculated using the lysimeter water balance (Schrader et al., 2013). The water balance equation for a lysimeter follows:

$$\Delta W = \text{AWI} - \text{ET}_a - D, \tag{1}$$
$$\text{AWI} = P + \text{NRW}, \tag{2}$$

where ΔW is the change in the lysimeter mass, AWI the atmospheric water input, ET_a the actual evapotranspiration, D the drainage, P the precipitation, and NRW non-rainfall water. The amount of precipitation is calculated from any increase in lysimeter mass after correction with water fluxes across the lysimeter bottom. It was assumed that no evaporation or transpiration occurred during the specific time period (Schneider et al., 2021; Schrader et al., 2013; Eq. 3). Any decrease in the lysimeter mass change after the correction with fluxes across the lysimeter bottom can thus be related to evapotranspiration if no precipitation occurred during this time interval (Eq. 4).

$$\text{AWI}_i = \begin{cases} \text{WL}_i - \text{WL}_{i-1} + \text{WT}_i - \text{WT}_{i-1} > 0 \\ 0 \text{ for } \text{WL}_i - \text{WL}_{i-1} + \text{WT}_i - \text{WT}_{i-1} \leq 0 \end{cases}, \tag{3}$$

$$\text{ET}_i = \begin{cases} -(\text{WL}_i - \text{WL}_{i-1} + \text{WT}_i - \text{WT}_{i-1}) \\ \text{ for } \text{WL}_i - \text{WL}_{i-1} + \text{WT}_i - \text{WT}_{i-1} < 0 \\ 0 \text{ for } \text{WL}_i - \text{WL}_{i-1} + \text{WT}_i - \text{WT}_{i-1} \geq 0 \end{cases}, \tag{4}$$

where AWI_i is the atmospheric water input during time interval i (kg), WL is the lysimeter mass in terms of the weight (kg), WT is the seepage tank weight (kg), and ET_i is the evapotranspiration amount during time interval i (kg).

2.2.2 Precipitation gauges

Two variants of the same tipping bucket gauge model (TB; ecoTech Umwelt-Meßsysteme GmbH, Bonn, Germany) are used at the test sites, which differ in the collecting surface of 200 cm² for SE and RO and 400 cm² for DD. The measuring mechanism is based on a funnel with an inlet water pipe. This leads the caught precipitation into a tipping bucket, which, when filled with a certain amount of water, tips to either side of the sharp edge pivot. The motion is determined by the weight imbalance caused by the water dripping from above. The device registers the number of tips with a magnet mounted on the bucket, inducing a signal to a reed switch. A second TB in RO and the TB in DD are additionally equipped with a heating module. The resolution of the TBs is 0.1 mm which indicates an equal volume of one of the buckets compartments.

The weighable gauge (WG) used in this study is the model Pluvio² manufactured by Ott Hydromet, Kempten, Germany. It uses load cells to determine the differences in weight in the weighing chamber caused by collected precipitation. The gauge has an orifice with a collecting area of 400 cm², a resolution of 0.01 mm, and a minimal cumulative precipitation threshold at 60 min collection time of 0.05 mm h⁻¹. The device outputs real-time and processed data with a time lag of a few minutes. A heating module is installed to prevent solid precipitation from blocking the gauge inlet. It merely heats the collecting ring around the orifice to avoid artificial loss due to evaporation. The model was used as a reference gauge in multiple studies (Johannsen et al., 2020; Kochendorfer et al., 2017a; Ryu et al., 2016) and was one of the most widely used WGs according to a survey within the WMO members in 2008 (Wong and Nitu, 2010). On the 19 July 2017, a single Alter wind shield was installed around the gauge in SE. This type of shield consists of loosely hanging lamellas, which are mounted on a concentric ring around the gauge (Alter,

1937), and is widely established to prevent wind loss and recommended by several institutes (Dengel et al., 2018).

The weather station WXT510 (Vaisala Oyi, Helsinki, Finland) is installed at all sites to measure meteorological standard parameters such as wind speed, wind direction, air temperature, relative humidity, and barometric pressure at 2 m height. The station includes the Vaisala RAINCAP® sensor, an acoustic sensor (AS) with a resolution of $0.01\,\mathrm{mm\,h^{-1}}$ (Salmi and Ikonen, 2005). The AS relies on a piezoelectric detector with a surface of $60\,\mathrm{cm^2}$, with which the impact of individual raindrops on the surface is measured. Raindrops collide with the surface at their terminal velocity, which is a function of the raindrop diameter. Depending on the terminal velocity and the mass of the raindrop, every collision creates a particular signal, which is proportional to the volume of the drops and is then converted to an individual voltage by the piezoelectric detector (Winder and Paulson, 2012). The voltage pulses are filtered, amplified, digitized, and analyzed. Knowing the voltage signals per unit time and the surface area and rain duration and intensity can be determined. Each type of precipitation creates a distinguishable signal, which enables the detection of liquid and solid precipitation. Since the terminal velocity of snow is low, the AS can only differentiate between rain and hail.

The laser disdrometer (LD; Adolf Thies GmbH & Co KG, Göttingen, Germany) is installed at the sites in RO and SE. The instruments use an infrared light beam with a wavelength of 780 nm and a cross section of approx. $46\,\mathrm{cm^2}$. It records the reduction in the transmitted light intensity by particles falling through the light beam and can therefore derive the particle diameter. The strength and duration of the attenuation initiated by the falling particle allows for an inference regarding its diameter and velocity, such that the precipitation type, rain and snow, can be distinguished (Bloemink and Lanzinger, 2005; Fehlmann et al., 2020). The LD distinguishes precipitation with a diameter of 0.125 mm and derives the vertical velocity by the measured signal duration (Lanzinger et al., 2006). It offers a low-sensitivity threshold with a resolution of $0.001\,\mathrm{mm\,h^{-1}}$.

Weather data as well as precipitation data from TB, WG, and AS are stored on a data logger at DD, RO, and SE (all "envilog Maxi", ecoTech, Bonn, Germany) at 10 min intervals (Pütz et al., 2016). Weighing data from the lysimeters are stored in a data logger (1 min intervals, DT85, Datataker-Thermo Fisher Scientific Australia Pty Ltd., Scoresby, VIC, Australia), whereas the LD's data are stored on a local memory card.

2.3 Data processing

Lysimeter data, which are available as time series of mass changes at a resolution of minutes, were pre-processed in four steps: (i) check of the monitored raw data time series', which is monitored by the minute, for plausibility (manually and automatically), (ii) application of the AWAT filter

to reduce the impact of noise on the raw data of the lysimeter mass changes (Peters et al., 2017), (iii) classification of $\mathrm{ET_a}$ and AWI data according to Eqs. (1)–(4) assuming that only $\mathrm{ET_a}$ or AWI can occur within the respective 1 min time step, and (iv) summing of the minute-based to hourly values; note that hours with missing values were marked as not available (NA).

Weather and gauge precipitation data were similarly treated with a plausibility check (manually and automatically) and an aggregation to hourly values. For this, the precipitation measurements present for 10 min intervals were summed, while the 10 min measurements from the climate stations such as temperature (°C), wind speed (m s^{-1}), and wind direction (°) were averaged over 1 h.

To determine whether the gauge data then add up to comparable hourly values and to be able to eliminate potential time lags between all devices, representative precipitation events were analyzed by comparing the 10 min with the hourly resolution (Appendix A1). Since the lysimeter measurements functioned as a reference for the comparison, they were intended to mark the beginning of an event as well as significant peaks within a precipitation event. The comparison revealed a time lag of 10 min between lysimeter and gauge data, which was due to time stamps from different data loggers. Another time lag for the WG data was induced by gauge-internal processing. Adjusting the overall gauge data with a 10 min inverse time lag and using the raw WG data solved the problem.

2.4 Reference precipitation values and their uncertainties

The derivation of a reference precipitation intensity (P_{ref}; mm h^{-1}) for the comparison of precipitation data is critical for further investigations. It was chosen to compute the mean measured precipitation among the lysimeters for each hourly data point (Eq. 5), when at least half of the lysimeters data were available for that hour. This way it is ensured that the mean is not dependent on single measurements and that too many data points are discarded because of missing values. At sites (SE and DD) where only three lysimeters of the same soil ecosystem are operated, the mean is calculated when at least two lysimeters provide measurements. The procedure is conducted for precipitation and NRW simultaneously; the following equations refer to the calculation of the reference precipitation, for which we only use AWI above 0.1 mm h^{-1}, which is assumed to be dominantly contributed by precipitation. The identification of non-rainfall water is covered in Sect. 2.5.1.

$$P_{\mathrm{ref}} = \begin{cases} \frac{1}{n}\sum_{i=1}^{n} x_i & \text{for } n \geq n_{\mathrm{na}} \\ \mathrm{NA} & \text{for } n < n_{\mathrm{na}} \end{cases}, \qquad (5)$$

where n is the number of lysimeters providing observations during time interval i (–), x_i the precipitation intensity mea-

sured by each lysimeter in the given interval i (mm h^{-1}), and n_{na} is the number of lysimeters with non-available data during time interval i (–).

Following WMO (2018), a rain intensity gauge is required to not exceed defined uncertainties while measuring rain precipitation intensities (P_{gauge}). Under field conditions, an uncertainty of 5 mm h^{-1} for $P_{gauge} < 100$ mm h^{-1} should not be exceeded. An approach conducted by Vuerich et al. (2009) derives P_{ref} from the mean of four different reference pit gauges. They calculated the uncertainty for the reference values from standard deviations of precipitation measurements from the pit gauges. The authors use the 95 % confidence level ($k = 2$) deducted from 2 times the standard deviation of the measurements. To adapt the concept, it was decided to proceed as follows: it is assumed that the aggregated hourly precipitation amounts determined by all available lysimeters are normally distributed around P_{ref}. Thus, the standard deviation (SD) between measurements of all lysimeters with the same vegetation cover at each site can be calculated for each hour, where data from all lysimeters is available (Eq. 6). After calculating the lysimeter uncertainties within the 95 % confidence level (U_{ref}; Eq. 7), each hour is assigned to a category according to its precipitation intensity value. Each category comprises a span of 0.1 mm h^{-1} for P_{ref} between 0 and P_{ref_max}, which was the maximum observed precipitation intensity during the observation period at each site – P_{ref_max}: 23.21 mm h^{-1} (RO); 12.91 mm h^{-1} (SE); 32.24 mm h^{-1} (DD). All uncertainty values for hours within the respective category are then averaged and the computed mean is attributed back to the respective hours. This assigns an individual uncertainty value to each precipitation intensity interval. The WMO (2018) recommends adding 5 % of P_{ref} to the gauge uncertainties (here lysimeter uncertainties; U_{fin}; Eq. 8) as an upper limit for uncertainties in rain gauges. The final uncertainties are then plotted and smoothed using the "geom_smooth" function (R, ggplot2 package; Wickham, 2016) with cubic splines using the R software (R Core Team, 2020) to provide an uncertainty range for the gauge comparison via scatterplots.

$$\text{SD} = \sqrt{\frac{\sum_{i=1}^{n}(x_i - x)^2}{n-1}}, \tag{6}$$

$$U_{ref} = P_{ref} \pm 2 \cdot \text{SD}, \tag{7}$$

$$U_{fin} = U_{ref} \pm 0.05 \cdot P_{ref}, \tag{8}$$

with n being the number of observations (–), x_i the precipitation intensities measured by each lysimeter during time interval i (mm h^{-1}), U_{ref} the empiric mean of the lysimeter measurements at the site during time interval i (mm h^{-1}), U_{ref} the uncertainty in the lysimeter reference during time interval i (mm h^{-1}), and U_{fin} the final uncertainty for the gauge comparison for time interval i (mm h^{-1}). To additionally reduce potential uncertainties and achieve more comparable results

when comparing the measurement methods with the lysimeter reference, only data are used for which P_{ref} and P_{gauge} are both ≥ 0.1 mm h^{-1}, which is the smallest common resolution of all measuring instruments.

2.5 Determination of key parameters

2.5.1 Non-rainfall water

Non-rainfall water (NRW) comprises the formation of dew, hoar frost, and fog. Often, combined observations by leaf wetness (for dew and hoar frost) or visibility sensors (fog) and weighable lysimeters are used to identify NRW (Zhang et al., 2019). No such sensors were available for our sites. Therefore, we followed the approach by Groh et al. (2018b); hourly precipitation data were categorized as NRW if no rain gauge except the lysimeters or the disdrometer registered precipitation. The disdrometer was excluded because it could detect fog. Additionally, the occurrence of NRW was limited to the period between sunset and sunrise, and the hourly NRW intensity was limited to a maximum rate of 0.07 mm h^{-1} according to assumptions on dew formation by Monteith and Unsworth (2013).

2.5.2 Precipitation type and intensity classification

The piezoelectric sensor as well as the optical disdrometer could identify the mentioned precipitation types in a sufficient way (Bloemink and Lanzinger, 2005; Fehlmann et al., 2020; Salmi and Ikonen, 2005). Due to an incomplete data situation, an approach was carried out to derive the precipitation type from the air temperature at the sites. For gauge intercomparisons, temperature ranges of +4 to 0 °C (Gebler et al., 2015), +2.5 to −2.5 °C (Kochendorfer et al., 2017b), +2 to 0 °C (Førland et al., 1996), and +2 to −2 °C (Ryu et al., 2016) were chosen for mixed precipitation. Here the latter threshold of +2 and −2 °C was used in this study for mixed precipitation (Table 2). Thus, temperatures above 2 °C are used to classify liquid precipitation (rain), and temperatures below −2 °C classify solid precipitation (snow). The small number of precipitation events classified as "snow" can be explained by the pre-filtering of the lysimeter measurements influenced by snow bridges or ice formation. Due to the small number of snow events and the uncertainties involved in quantifying snow and mixed precipitation with lysimeters and precipitation gauges, hours within both categories are excluded from further investigation.

The precipitation intensities were classified according to WMO (2018). Here, observations were classified according to the precipitation registered by the lysimeter reference. Hours with $0.1 \leq P_{ref} < 2.5$ mm h^{-1} were regarded as "slight", $2.5 \leq P_{ref} < 10$ mm h^{-1} as "moderate", and $10 \leq P_{ref} < 50$ mm h^{-1} as "heavy" rainfall (Table 2). More details on the precipitation intensity distributions are provided in Appendix B1 and B2.

Table 2. Number of hours classified according to the reference rain intensity (P_{ref}) and number of hours with precipitation classified as "mixed" and "snow" for the years 2015–2018. Hours for which no reference could be calculated due to missing data and hours with $P_{\text{ref}} < 0.1$ are excluded.

Site	Slight rain $(0.1 \le P_{\text{ref}} < 2.5\,\text{mm}\,\text{h}^{-1})$ (h)	Moderate rain $(2.5 \le P_{\text{ref}} < 10\,\text{mm}\,\text{h}^{-1})$ (h)	Heavy rain $(10 \le P_{\text{ref}} < 50\,\text{mm}\,\text{h}^{-1})$ (h)	Mixed $(0.1 \le P_{\text{ref}} < 50\,\text{mm}\,\text{h}^{-1})$ (h)	Snow (h)
Rollesbroich	3338	257	1010	639	26
Selhausen	2675	160	4	146	9
Dedelow	2047	127	4	261	14

2.6 Correlation analyses

The precipitation measurements between the reference values and those obtained from the gauges were compared based on x–y scatterplots (e.g., Haselow et al., 2019; Liu et al., 2013; Yang, 2014). Within a plot, the uncertainty range, the bias (Eq. 9) as well as the standard deviation of the measurement differences (SDDs, Eq. 10), the R^2 value (Eq. 11), the number of observations (n), and the linear regression line (Eq. 12) are given. To enhance the visualization, additional plots and statistics for slight precipitation events are provided.

$$\text{Bias} = \sum_{i=1}^{n} \frac{(x_i - y_i)}{n}, \quad (9)$$

$$\text{SDD} = \sqrt{\frac{\sum_{i=1}^{n} (x_i - y_i)^2}{n - 1}}, \quad (10)$$

$$R^2 = \frac{\sum (y_i - \overline{x})^2}{\sum x_i - \overline{x}} \text{ with } \overline{x} = \frac{1}{n} \sum_{i=1}^{n} x_i, \quad (11)$$

where n is the number of observations (–), x_i the reference precipitation intensity during time interval i (mm h^{-1}), and y_i the precipitation intensity determined by the precipitation gauge during time interval i (mm h^{-1}).

The bias is the average difference between the precipitation measured by the gauge and the reference measurement, so positive or negative values indicate that the gauges generally over- or underestimated precipitation, respectively. The SDD quantifies the distribution of the differences and thus the spread of the data points around the 1 : 1 reference line. The nondimensional coefficient of determination, R^2, describes how well the linear regression model, displayed in the plot, fits the data. Due to its derivation, it is also closely related to the extent of the spread of the data but does not consider the spread around the 1 : 1 reference line. The regression lines follow the standard linear regression (Eq. 12) performed in R (R Core Team, 2020), using the ggplot2 package (Wickham, 2016).

$$y_i = \alpha + \beta x_i, \quad (12)$$

where α and β are regression coefficients.

While interpreting the bias, SDD, R^2 value, and regression lines, it must be considered that these statistics and methods are based on the assumption of normally distributed data. Precipitation data do not follow such a distribution. Low precipitation intensities occur more often than higher intensities and therefore the residuals are heteroscedastic. Thus, the statistics might not be enough to describe the data distribution. An additional, visual illustration of the data was required, as presented by the scatterplots.

2.7 Wind error analysis

To analyze the influence of wind speed at gauge height (v_{g}) on the gauge's precipitation measurements, the catch ratio (CR; Eq. 13) is used. The CR can be described as a function of wind speed and temperature (Goodison et al., 1998; Yang et al., 1998). CRs of different gauges were calculated with regression analyses on the basis of reference measurements at multiple sites (Chen et al., 2015; Goodison et al., 1998; Sugiura et al., 2006; Yang et al., 2000). The CR of a gauge and reference values can also be described with the following equation:

$$\text{CR} = \frac{P_{\text{gauge}}}{P_{\text{ref}}} \cdot 100. \quad (13)$$

Since the influence of the temperature can be neglected due to the exclusion of mixed and solid precipitation, the primary parameter to consider is the wind speed at gauge height, which can be derived from the measured wind speed at 2 m above the ground (Eq. 14; Goodison et al., 1998):

$$v_{\text{g}} = \frac{\log\left(\frac{h_{\text{g}}}{z_0}\right)}{\log\left(\frac{h}{z_0}\right)} \cdot v_{\text{h}}, \quad (14)$$

where v_{g} is the wind speed at the height of the gauge orifice (m s^{-1}), h_{g} the height of the gauge orifice above the ground (m), z_0 the roughness length (0.01 m in winter, 0.03 m in summer), h the height of the wind speed measuring instrument above the ground (m), and v_{h} the wind speed measured by the measuring instrument (m s^{-1}). The CRs of each gauge were binned according to the site-specific ranges of v_{g} with each bin representing an interval of 0.1 m s^{-1} and then aver-

Table 3. Wetting and gauge constants for Eq. (16) provided by Michelson (2004) for multiple gauge types. SMHI: gauge used by the Swedish Meteorological and Hydrological Institute.

Precipitation phase	Constant	SMHI ($\text{mm} \, 12 \, \text{h}^{-1}$)	Hellmann ($\text{mm} \, 12 \, \text{h}^{-1}$)
Liquid	Gauge	−0.05	0.00
Liquid	Wetting	0.07	0.14

Table 4. Daily evaporation loss constants for Eq. (16) as provided by Michelson (2004) for the Hellmann-type gauge.

Month	Hellmann ($\text{mm} \, 12 \, \text{h}^{-1}$)
January	0.01
February	0.02
March	0.03
April	0.04
May	0.09
June	0.15
July	0.16
August	0.08
September	0.02
October	0.01
November	0.01
December	0.01

aged within the bin to reduce the overall amounts of observations and identify possible trends.

2.8 Precipitation data corrections

Sevruk (1982) provides a general equation for the correction of precipitation measurements which is adjusted with regard to an improved readability to the notation by Førland et al. (1996; Eq. 15):

$$P_{\text{cor}} = k \, (P_{\text{m}} + P_{\text{w}} + P_{\text{e}} + P_{\text{t}}), \tag{15}$$

with P_{cor} being the corrected precipitation (mm), k the correction factor for wind (–), P_{m} the measured precipitation (mm), P_{w} the wetting loss (mm), P_{e} the evaporation loss (mm), and P_{t} the loss by trace precipitation (mm).

Few of the correction methods based on Eq. (15) are developed to correct precipitation measurements on an hourly basis, due to the absence or small numbers of automatic gauge types in the last decades. Førland et al. (1996) published the dynamic correction model (DCM) with which Michelson (2004) corrected hourly precipitation data from four different gauge models mainly used in Scandinavian countries. The correction factor for wind loss, k, can thus be adjusted for hourly rain measurements following the DCM (Førland et al., 1996; Michelson, 2004; Eq. 16):

$$k = \exp \left[\begin{array}{l} -0.00101 \cdot \ln\left(P_{\text{gauge}}\right) - 0.012177 \cdot v_{\text{g}} \\ \cdot \ln\left(P_{\text{gauge}}\right) + 0.034331 \cdot v_{\text{g}} + 0.007697 + c \end{array} \right], \tag{16}$$

where c is the gauge constant ($\text{mm} \, 12 \, \text{h}^{-1}$).

Michelson (2004) offers empiric constants for wetting loss, evaporation loss, and the wind-induced error for four different gauge models and precipitation types (Tables 3 and 4). The empiric constants apply for 12 h measuring intervals, which can be derived on an hourly basis. Since evaporation does not account for WGs if it is suppressed with an oil film (WMO, 2008), only the gauge constant for determining the wind error has to be chosen for the WG. Michelson (2004) states that precipitation gauge designs that are similar to the WG used here have a slightly improved gauge constant compared to the Hellmann gauge (0.0 $\text{mm} \, 12 \, \text{h}^{-1}$), thus a gauge constant of −0.05 $\text{mm} \, 12 \, \text{h}^{-1}$ is chosen for the WG.

To compensate for the loss by trace precipitation for the TB, an empiric value provided by Yang et al. (2001) with a loss of 0.1 $\text{mm} \, \text{d}^{-1}$ is assumed for days with at least one precipitation event.

Richter (1995) developed a correction method especially for German Hellmann-type gauges installed at sites where no wind speed can be determined. He used factors depending on the shielding of the site and the precipitation type, based on long-term precipitation measurements. The derived daily correction amount includes all relevant losses (including wind, evaporation, trace, and wetting). To test the potential of the correction method by Richter (1995) to be applied to hourly precipitation data, a similar approach to the one published by Gebler et al. (2017) is chosen. The authors initially calculated corrections for daily precipitation data according to Richter (1995; Eqs. 17 and 18) and then redistributed them to hourly measurements via the ratio of daily measured to daily corrected data. Here it was decided to redistribute the daily corrections via the number of precipitation hours within a day (Eq. 19):

$$P_{\text{d}}^{\text{cor}} = P_{\text{d}} + \Delta P_{\text{d}}, \tag{17}$$

$$\Delta P_{\text{d}} = b \cdot P_{\text{d}}^{\varepsilon}, \tag{18}$$

$$P_{\text{h}}^{\text{cor}} = \frac{P_{\text{d}}^{\text{cor}}}{n_{\text{Pevent}}} + P_{\text{h}}, \tag{19}$$

where $P_{\text{d}}^{\text{cor}}$ is the corrected daily precipitation ($\text{mm} \, \text{d}^{-1}$), P_{d} the daily precipitation measured by a gauge ($\text{mm} \, \text{d}^{-1}$), ΔP_{d} the amount of daily additional precipitation ($\text{mm} \, \text{d}^{-1}$), b the coefficient for the influence of wind exposition at the measurements site (–), $P_{\text{d}}^{\varepsilon}$ the empiric coefficient for the precipitation type (–), $P_{\text{h}}^{\text{cor}}$ the corrected hourly precipitation ($\text{mm} \, \text{h}^{-1}$), n_{Pevent} the number of hours with $P_{\text{ref}} \geq 0.1 \, \text{mm} \, \text{h}^{-1}$ within a day (–) and P_{h} the hourly precipitation measured by the gauge ($\text{mm} \, \text{h}^{-1}$).
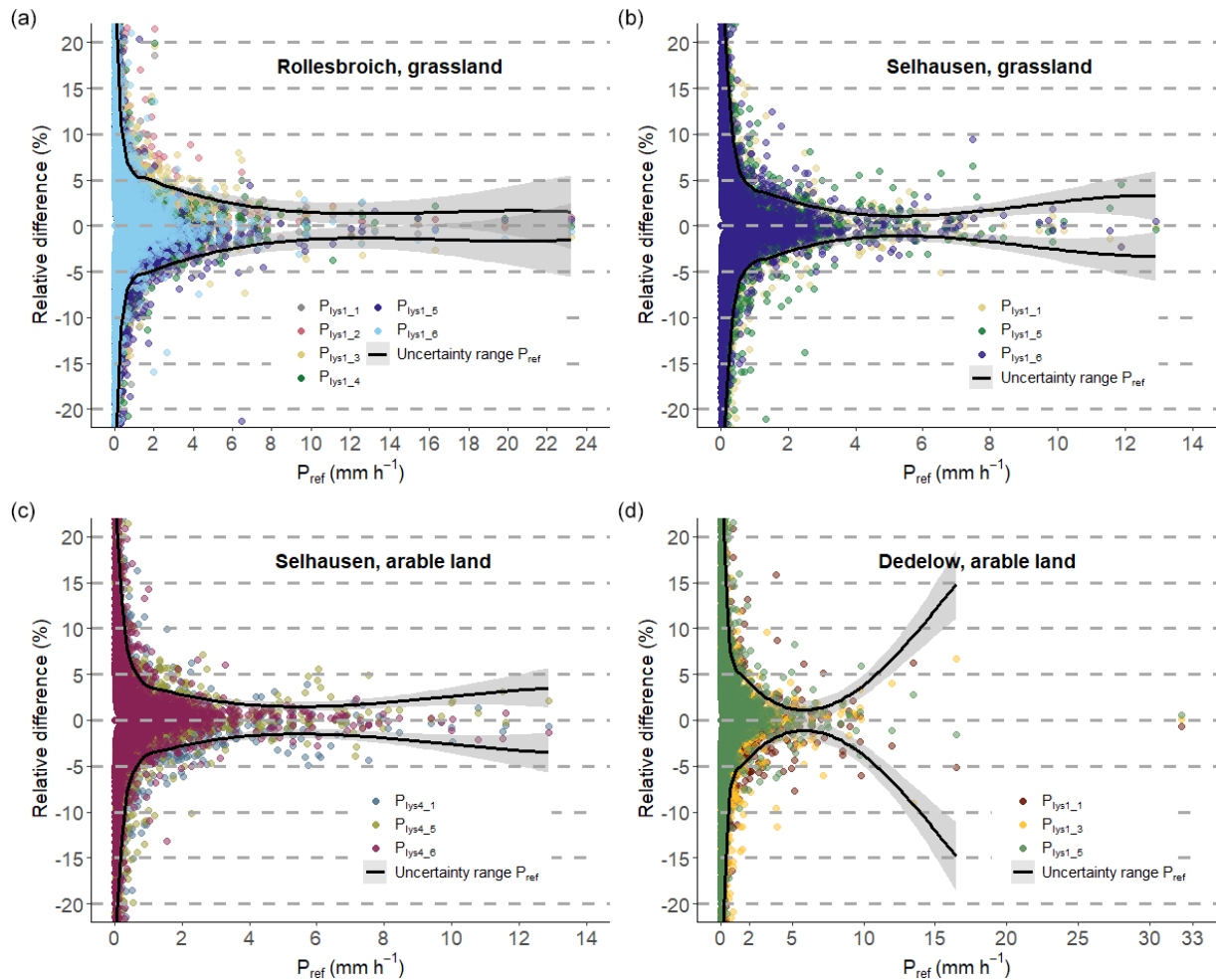
Figure 3. Uncertainty ranges of lysimeter references (P_{ref}), delimited through solid lines, and differences in each lysimeter measurement relative to P_{ref}. **(a)** Rollesbroich lysimeter station; lysimeter with grassland. **(b)** Selhausen lysimeter station; lysimeter with grassland. **(c)** Selhausen lysimeter station; lysimeter with arable land. **(d)** Dedelow lysimeter station; lysimeter with arable land.

3   Results

3.1   Uncertainty range of the lysimeters

With increasing P_{ref} values, the measurement uncertainties from the lysimeters decrease at all sites. The uncertainty ranges indicate that between 1 and 2.5 mm h^{-1} the relative measurement differences decrease to values below 5 % (Fig. 3). For $P_{ref} > 8$ mm h^{-1}, the lack of data does not allow us to delineate a clear area of uncertainty. In DD, three rain events with precipitation intensities > 11 mm h^{-1} were associated with increased deviations within the lysimeter measurements, which bias the regression line and therefore the predicted uncertainty range at these precipitation intensities (Fig. 3d).

3.2   Annual precipitation values

During hours in which all devices at a site were available and at least one gauge (TB, WG or AS) and the lysimeters measured a precipitation intensity of 0.1 mm h^{-1} or higher (Table 5), the TB1 in Rollesbroich (RO) registered 22.9 %–47.1 % of P_{ref} within each individual year of operation. The TB in Selhausen (SE) caught 20.4 %–40.7 %, TB2 (RO) caught 79.2 %–83.8 %, and the TB in Dedelow (DD) caught 72.8 %–84.0 %. The WGs caught 82.2 %–89.0 % (RO) and 89.4 %–94.5 % (SE). The AS measured 62.8 %–78.2 % (RO), 70.0 %–82.1 % (SE), and 82.6 %–91.3 % (DD). The LD (RO) measured 85.7 %–95.3 %, while the LD (SE) measured 73.6 %–96.1 %. Deviations between the precipitation totals of the lysimeters with different vegetation cover in SE are considerably low with CRs of 99.8 %–101.4 %.

Table 5. Precipitation sums (P) and catching ratios (CRs) of all investigated gauges compared to the references per year. Only hours are considered where all devices at a site were active; at least one device, tipping bucket (TB), weighable gauge (WG), or acoustic sensor (AS), and the lysimeters measured a precipitation intensity of at least 0.1 mm h^{-1}; and the precipitation is classified as "rain".

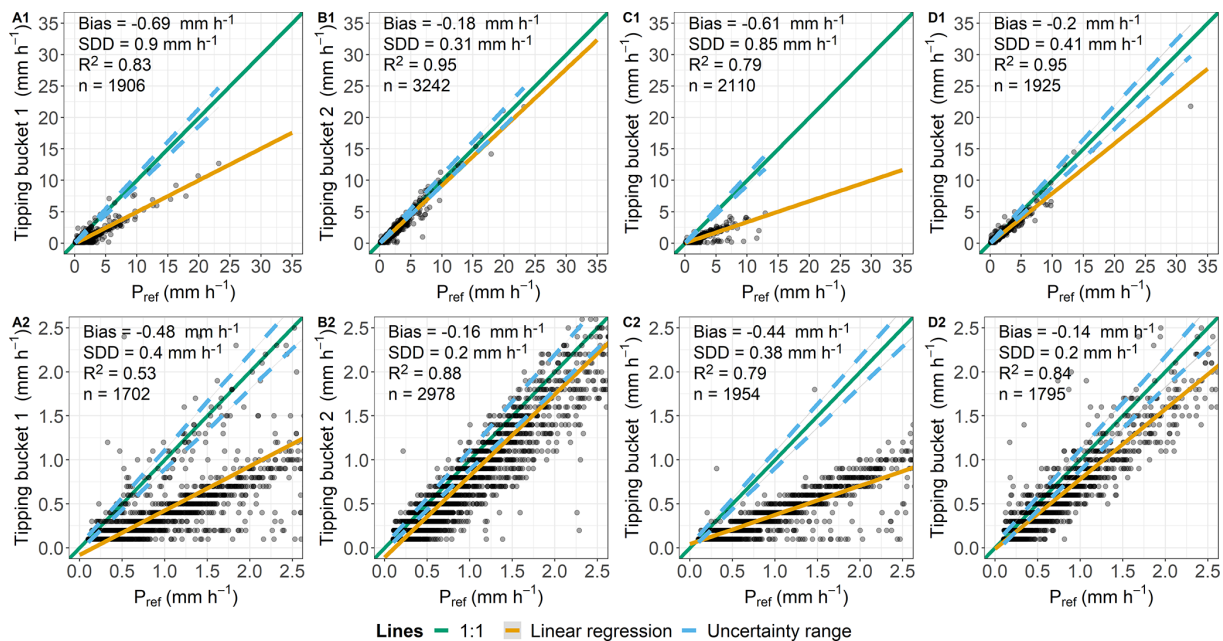| Site	Year (–)	n (h)	P_{ref} (mm)	P_{lys_crop} (mm)	CR_{lys_crop} (%)	P_{TB1} (mm)	CR_{TB1} (%)	P_{TB2} (mm)	CR_{TB2} (%)	P_{WG} (mm)	CR_{WG} (%)	P_{AS} (mm)	CR_{AS} (%)	P_{LD} (mm)	CR_{LD} (%)
Rollesbroich	2015	793	709			334	47.1	594	83.8	606	85.5	499	70.4	676	95.3
	2016	989	801			184	22.9	634	79.2	659	82.2	526	65.6	687	85.7
	2017	1007	881			273	30.9	732	83.1	744	84.5	553	62.8	795	90.2
	2018	694	583			189	32.4	471	80.8	519	89.0	456	78.2	522	89.6
Selhausen	2015	736	599	600	100.1	244	40.7			549	91.7	423	70.6	589	98.4
	2016	697	554	556	100.3	221	39.9			495	89.4	388	70.0	455	82.1
	2017	581	431	430	99.8	169	39.2			398	92.3	303	70.2	317	73.6
	2018	548	388	394	101.4	79	20.4			367	94.5	319	82.1	373	96.1
Dedelow	2015	571	414			344	83.1					373	90.1		
	2016	641	423			322	76.1					351	83.1		
	2017	719	693			504	72.8					572	82.6		
	2018	407	279			235	84.0					255	91.3		

Figure 4. Comparison of hourly data determined by tipping buckets and lysimeters (P_{ref}) and classified as "rain". Plots **(A1)–(D1)** include all measurements taken where both P_{gauge} and P_{ref} are ≥ 0.1 mm h^{-1}. Plots **(A2)–(D2)** show slight precipitation events, and key values are calculated for P_{ref} between 0.1–2.5 mm h^{-1}. **(A1, A2)** Rollesbroich lysimeter station. **(B1, B2)** Rollesbroich eddy covariance (EC) station. **(C1, C2)** Selhausen lysimeter station. **(D1, D2)** Dedelow lysimeter station.

3.3 Precipitation intensities

On an hourly basis, all TBs tend to underestimate precipitation relative to the reference (Fig. 4). Measurements of the TBs showed little scattering, indicating consistent measurements with R^2 values above or near 0.8 for all devices, except for TB1 in RO (Fig. 4A2) with $R^2 = 0.53$. However, TB1 (RO; Fig. 4A1) as well as the TB (SE; Fig. 4C1) showed biases of -0.69 and -0.61 mm h^{-1} and SDDs of 0.90 and 0.85 mm h^{-1} for all rainfall events with $P_{ref} \geq 0.1$ mm h^{-1}. In hours of intensities between 0.1 to 2.5 mm h^{-1}, the biases

were -0.48 and -0.44 mm h^{-1} and the SDDs were 0.40 and 0.38 mm h^{-1} (Fig. 4A2 and C2). Measurements from TB2 (RO; Fig. 4B1) showed a bias of -0.18 mm h^{-1} and an SDD of 0.31 mm h^{-1}, while the TB (DD; Fig. 4D1) measured with a bias of -0.20 mm h^{-1} and an SDD of 0.41 mm h^{-1}. For slight precipitation intensities, measurements from TB2 (RO) had a bias of -0.16 mm h^{-1} and an SDD of 0.20 mm h^{-1} and TB (DD) had a bias of -0.14 mm h^{-1} and an SDD of 0.2 mm h^{-1} (Fig. 4B2 and D2).

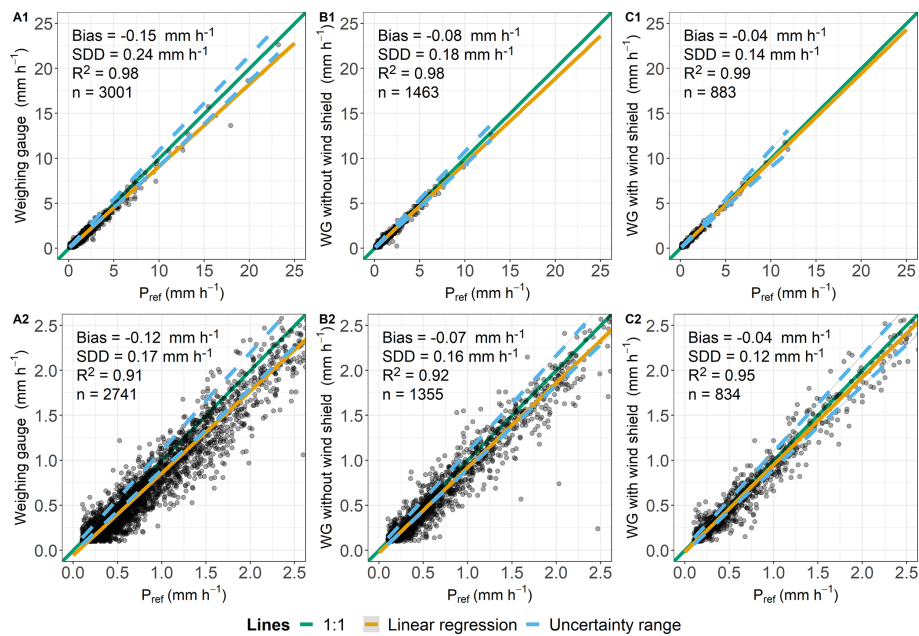Measurements conducted by the WG (RO; Fig. 5A1) showed a bias of -0.15 mm h^{-1} and an SDD of

Figure 5. Comparison of hourly data determined by weighable gauges and lysimeters (P_{ref}) and classified as "rain". Plots **(A1)**–**(C1)** include all measurements taken where both P_{gauge} and P_{ref} are $\geq 0.1 \, \text{mm h}^{-1}$. Plots **(A2)**–**(C2)** show slight precipitation events, and key values are calculated for P_{ref} between 0.1–2.5 mm h^{-1}. **(A1, A2)** Rollesbroich lysimeter station. **(B1, B2)** Selhausen lysimeter station without installed wind shield around the weighable gauge. **(C1, C2)** Selhausen lysimeter station with installed wind shield around the weighable gauge.

0.24 mm h^{-1}. For the time without a wind shield, measurements from the WG (SE; Fig. 5B1) had a bias of $-0.08 \, \text{mm h}^{-1}$ and an SDD of 0.18 mm h^{-1}, while with a shield the bias was $-0.04 \, \text{mm h}^{-1}$ and the SDD 0.14 mm h^{-1} (Fig. 5C1). At $P_{ref} \leq 2.5 \, \text{mm h}^{-1}$, the bias decreased from 0.07 to 0.04 mm h^{-1} and the SDD from 0.16 to 0.12 mm h^{-1} after the installation of the wind shield (Fig. 5B2 and C2) in comparison with the WG (RO; Fig. 5A2), the measurements of which for $P_{ref} \leq 2.5 \, \text{mm h}^{-1}$ had a bias of $-0.11 \, \text{mm h}^{-1}$ and an SDD of 0.16 mm h^{-1}.

The AS data scattered largely around the 1 : 1 line with the tendency of the ASs to underestimate the precipitation intensity (Fig. 6A1 to C2). For slight precipitation intensities, in particular, the measurements correlated poorly with the reference data. To exclude possible errors during the data processing, hourly values were calculated additionally, implementing a positive and negative 10 min lag in the data. This led to an even lower degree of agreement with the reference measurements, resulting in higher bias and SDDs than shown in Fig. 6. Additionally, a discrepancy between the measurement intervals from the ASs and reference would also result in false positives because only sensor data would show precipitation. A plot with the data including $P_{ref} = 0$ (not shown here) reveals no suspicious occurrence of these false positives. Therefore, the data from the ASs was evaluated as valid. Measurements from the AS (RO; Fig. 6A1) had a bias of $-0.25 \, \text{mm h}^{-1}$ and an SDD of 0.7 mm h^{-1}. A bias of $-0.22 \, \text{mm h}^{-1}$ and an

SDD of 0.46 mm h^{-1} were calculated for $P_{ref} \leq 2.5 \, \text{mm h}^{-1}$ (Fig. 6A2). The R^2 value was 0.80 and 0.54. Measurements by the AS (SE) had a bias of $-0.23 \, \text{mm h}^{-1}$, an SDD of 0.57 mm h^{-1}, and an R^2 value of 0.79 (Fig. 6B1). For intensities classified as slight, the sensor measured with a bias of $-0.18 \, \text{mm h}^{-1}$, an SDD of 0.37 mm h^{-1}, and an R^2 value of 0.62 (Fig. 6B2). The measurements from the AS in DD had a bias of 0.07 mm h^{-1} and an SDD of 0.66 mm h^{-1}, with R^2 being 0.85 (Fig. 6C1). Slight precipitation was measured with a bias of $-0.07 \, \text{mm h}^{-1}$, an SDD of 0.42 mm h^{-1}, and an R^2 value of 0.60 (Fig. 6C2).

The LD (RO) tended to overestimate the precipitation with a general bias of 0.01 mm h^{-1} and an SDD of 0.37 mm h^{-1} (Fig. 7A1). The R^2 value of 0.95 suggests a good correlation with the reference. For slight precipitation events, the bias was 0.00 mm h^{-1}, with the SDD being 0.18 mm h^{-1} and R^2 0.90 (Fig. 7A2).

The LD (SE) showed biases of 0.02 mm h^{-1} for all measurements and 0.04 mm h^{-1} for $P_{ref} < 2.50 \, \text{mm h}^{-1}$ (Fig. 7B1 and B2). The SDDs were 0.61 and 0.43 mm h^{-1}. The R^2 values (0.75 and 0.58) were lower compared to the ones from the other disdrometer at RO. The number of recorded hours with precipitation occurring at both sides was higher for the plots with the disdrometers compared to the plots of the other gauges due to the high measuring resolution of the disdrometer.
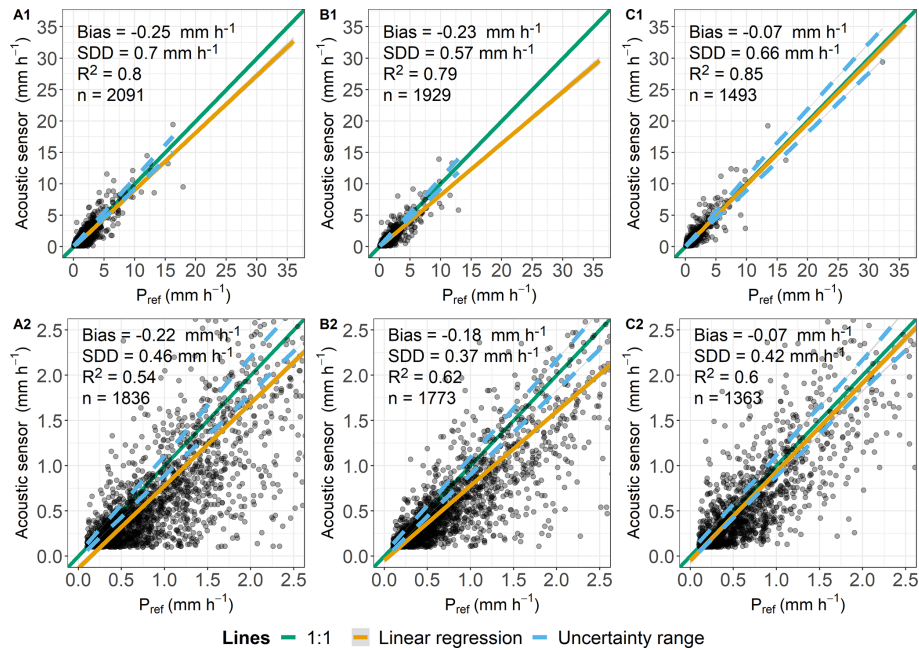
Figure 6. Comparison of hourly data determined by acoustic sensors and lysimeters (P_{ref}) and classified as "rain". Plots **(A1)–(C1)** include all measurements taken where both P_{gauge} and P_{ref} are $\geq 0.1\,\mathrm{mm\,h^{-1}}$. Plots **(A2)–(C2)** show slight precipitation events, and key values are calculated for P_{ref} between 0.1–2.5 mm h^{-1}. **(A1, A2)** Rollesbroich lysimeter station. **(B1, B2)** Selhausen lysimeter station. **(C1, C2)** Dedelow lysimeter station.

3.4 Influence of wind speed

The CRs from TB1 (RO) and TB (SE) as functions of the wind speed at gauge height were mostly in the range of 30 %–100 % (Fig. 8a and c). CRs of TB1 (RO) show higher values for wind speeds above 8 m s^{-1}, while those from TB (SE) did not increase or decrease with increasing wind speed at gauge height. The CRs from TB2 (RO) showed a tendency to decrease at higher wind speeds (Fig. 8b). In contrast, the CRs from TB (DD) tended to be above 100 % after exceeding wind speeds of 6 m s^{-1}, and the regression line implied a positive correlation with the wind speed (Fig. 8d). The CRs from the WGs did not exhibit any correlation between the hourly precipitation data and the wind speed (Fig. 9a to c), except for WG (SE) without a wind shield, for which the CRs tended to decrease with increasing wind speed.

At all sites, the CRs of the ASs increased with higher wind speeds (Fig. 10a to c). The CRs of the LDs also indicated slight dependencies on the wind speed at gauge height (Fig. 11a and b), while the CRs of the LD in SE generally spread to a greater extent around the 100 % reference line compared to LD in RO.

3.5 Precipitation correction

Applying the dynamic correction model (DCM) and the approach derived from Richter (1995) reduced the bias of all corrected measurements for the TBs and WGs (Table 6).

Generally, the DCM resulted in a greater bias reduction than the other method. Neither correction method had a systematic effect on the SDD and R^2 values, but the CRs increased by 14 % and 9 % for the TBs and by 10 % and 11 % for the WGs due to the application of the DCM and method after Richter, respectively. The data correction also led to an increased number of hours exceeding the threshold of 0.1 mm h^{-1} for the WGs (Tables 6 and 7). For the TBs, the aggregation of hourly to daily precipitation data during a processing step of the method derived from Richter resulted in a reduction in observations.

4 Discussion

4.1 Lysimeter measurements, reference values, and the influence of non-rainfall water

The uncertainty ranges of the reference values and the overall strong correlation between the measurements of the lysimeters within a site (Appendices C1–3 and D1) demonstrate that under field conditions and at different locations, the lysimeter measurements were in good agreement with each other over the entire observation period at all sites. The uncertainties in the reference values meet the requirements defined by the WMO (2018) for gauges used in the field. They decreased with increasing precipitation intensity, reaching a threshold of 5 % at about 1 to 2 mm h^{-1}, which was observed at all study sites and regardless of the vegetation cover of the

Table 6. Statistics of the corrected precipitation data classified as "rain" for tipping bucket (TB) and weighable gauges (WG) at sites in Rollesbroich (RO), Selhausen (SE), and Dedelow (DD). The number of observations (n) varied depending on the correction method due to hourly value aggregation and the presence of incomplete data as well as the 0.1 mm h^{-1} threshold, which was only met after the correction. "Intercept" and "slope" show the intercept and slope of the linear regression of P_{gauge} and P_{ref}.

Site	Device	Corr. method	Intercept (mm h^{-1})	Slope (–)	Bias (mm h^{-1})	SDD (mm h^{-1})	R^2 (–)	n (–)
Rollesbroich	TB1	–	−0.08	0.50	−0.69	0.90	0.83	1906
	TB1	DCM	−0.01	0.47	−0.56	0.88	0.82	1906
	TB1	Richter	0.00	0.51	−0.61	0.90	0.83	1831
	TB2	–	−0.11	0.93	−0.18	0.31	0.95	3242
	TB2	DCM	0.01	0.96	−0.03	0.30	0.95	3242
	TB2	Richter	−0.03	0.94	−0.09	0.30	0.95	3224
Selhausen	TB	–	−0.04	0.33	−0.61	0.85	0.79	2110
	TB	DCM	0.13	0.35	−0.51	0.83	0.78	2110
	TB	Richter	0.11	0.34	−0.54	0.85	0.78	2019
Dedelow	TB	–	−0.01	0.79	−0.20	0.41	0.95	1925
	TB	DCM	0.11	0.81	−0.06	0.42	0.93	1925
	TB	Richter	0.07	0.80	−0.11	0.41	0.94	1925
Rollesbroich	WG	–	−0.06	0.91	−0.15	0.24	0.98	3001
	WG	DCM	0.01	0.95	−0.04	0.22	0.98	3107
	WG	Richter	0.01	0.93	−0.06	0.23	0.98	3185
Selhausen	WG	–	−0.02	0.95	−0.07	0.17	0.98	2346
	WG	DCM	0.01	0.99	0.01	0.17	0.98	2439
	WG	Richter	0.05	0.97	0.03	0.16	0.98	2497

Table 7. Catching ratios (CRs) of corrected tipping bucket (TB) and weighable gauge (WG) data (DCM: dynamic correction model; RI: correction based on the method derived from Richter, 1995). Only the numbers (n) of hours are considered when all devices at a site were active and at least one device (TB, WG, AS) measured precipitation (P) classified as "rain" of at least 0.1 mm h^{-1}. The latter conditions are met differently after the correction with the two correction methods, resulting in divergent numbers of observations and associated P_{ref}.

Site	Year (–)	n DCM (h)	n RI (h)	P_{ref} DCM (mm)	P_{ref} RI (mm)	CR_{TB1} DCM (%)	CR_{TB1} RI (%)	CR_{TB2} DCM (%)	CR_{TB2} RI (%)	CR_{WG} DCM (%)	CR_{WG} RI (%)
Rollesbroich	2015	799	801	710	693	57.8	53.0	99.9	92.2	97.4	94.0
	2016	1009	1054	803	805	29.5	26.9	95.0	88.7	92.4	92.0
	2017	1027	1020	882	856	39.6	36.5	98.3	93.0	94.7	94.0
	2018	709	705	584	557	41.3	38.0	96.3	90.8	99.7	99.1
Selhausen	2015	760	744	601.36	552.4	52.5	48.9			100.5	103.7
	2016	721	733	556.31	529	51.4	48.1			97.3	100.8
	2017	598	616	432.88	411.6	51.3	48.0			99.6	105.5
	2018	570	611	389.81	391.6	28.8	25.8			104.5	107.5
Dedelow	2015	571	571	407.52	407.5	103.3	97.2				
	2016	641	641	410.68	410.7	97.2	91.8				
	2017	719	719	682.1	682.1	87.5	83.1				
	2018	407	407	271.31	271.3	106.7	100.9				

lysimeters. Additionally, lysimeter data at the sites showed R^2 values of 1 with a maximum bias of 0.01 mm h^{-1} and a maximum SDD of 0.05 mm h^{-1} (Appendix C1 to C3), indicating a good correlation. Since lysimeter measurement uncertainties increase exponentially with decreasing precipita-

tion intensity from $P_{\text{ref}} < 1$ mm h^{-1}, calculating an average intensity from multiple lysimeters seems necessary for these data. For long-term periods, uncertainties were probably less important because of the assumed normally distributed deviations from the average. A relevant influence of the spatial
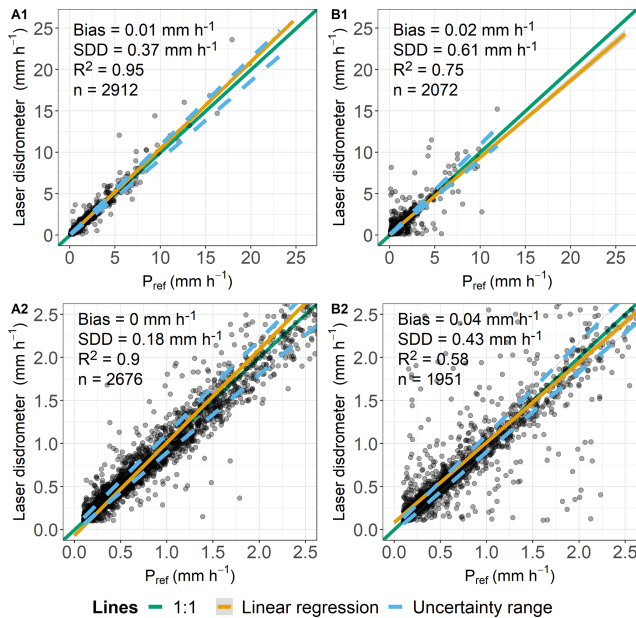
Figure 7. Comparison of hourly data determined by laser disdrometer and lysimeters (P_{ref}) and classified as "rain". Plots **(A1)**–**(B1)** include all measurements taken with both P_{gauge} and P_{ref} being $\geq 0.1\,mm\,h^{-1}$. Plots **(A2)**–**(B2)** show slight precipitation events, and key values are calculated for P_{ref} between 0.1–2.5 $mm\,h^{-1}$. **(A1, A2)** Rollesbroich lysimeter station. **(B1, B2)** Selhausen lysimeter station.

autocorrelation of precipitation was not found, which might go back to the temporal resolution of the data, the uniform environment without shielding, and the overall small areas covered by the lysimeters and measuring methods.

In total, when comparing the cumulated precipitation within a certain period, the lysimeters registered more precipitation than any other precipitation gauge. It could therefore be assumed that the lysimeter measurements and therefore the reference values are closer to the actual precipitation than any of the other measurement methods compared. The results therefore also indicate that the procedure to distinguish between water loss by ET and water input by AWI on a basis of minutes prevented the significant loss of registered AWI due to ET. However, comparing total precipitation amounts over long-term periods between the gauges and lysimeters, even if filtered carefully, might be biased because of non-rainfall water (NRW), which contributed to the recorded precipitation measured by the lysimeters. NRW which deposited before, during, or after a regular precipitation event within a respective time interval was hence classified as precipitation, while other precipitation gauges did not record this. NRW could thus lead to overestimations of lysimeter precipitation intensities, although the average NRW intensity (RO: 0.011 $mm\,h^{-1}$; SE: 0.009 $mm\,h^{-1}$; DD: 0.012 $mm\,h^{-1}$; Appendix E1) was small compared to the precipitation intensity and the distribution of NRW in-

tensities (Fig. 12a to c) indicated that these presumably did not heavily bias hours with regular precipitation. Applying these averages for NRW intensities to all hours which were investigated for the comparison of precipitation totals (Table 5), only 1.3 % (RO), 1.2 % (SE), and 1.6 % (DD) of the total registered precipitation would have been attributed to NRW. This indicates a possibly small impact of NRW on the results of this study. However, NRW (i.e., dew, hoar frost, and fog) can contribute a substantial amount of water to the ecosystem at the annual scale (Forstner et al., 2021; Groh et al., 2019), which demonstrates clearly that high-precision lysimeters are ideal tools for measuring different NRW of ecosystems. A higher temporal resolution of the data, possibly at 10 min intervals, could help to temporally delineate precipitation events and NRW, as used by Groh et al. (2018b).

4.2 Evaluation of gauge types for the comparison of precipitation data

The systematic deviations between the reference values and the precipitation intensity measurements by TB1 in RO (Fig. 4a) and the TB in SE (Fig. 4c) on one hand and the better-fitting data from TB2 (RO; Fig. 5b) and TB in DD (Fig. 4d) on the other hand can only be explained by divergent calibrations. All TBs were of the same type and only differed in the equipped heating module. This did not affect the measurements compared, since the module only worked at low temperatures and was intended to melt solid precipitation. The TB (DD) also had a greater catching surface area of 400 cm^2 compared to 200 cm^2 at other sites. However, this effect should be deducted by the internal processing. A spatial influence on the measurements was also unlikely since TB2 in RO was installed 30 m away from the lysimeter station and measured values closer to the reference than TB1, which was located only 5 m beside the lysimeters. The maintenance and service intervals were nearly equal at all sites. No or incorrect calibration could lead to a systematic underestimation of precipitation measurements, especially regarding TBs (Calder and Kidd, 1978; Niemczynowicz, 1986; Shedekar et al., 2016). If the precipitation amount of the internal processing software does not agree with the amount of liquid, which is poured by a tip of the bucket, the bias increases with the numbers of tips. Thus, an increased underestimation of the precipitation intensity can be recognized with increasing reference values. Kohfahl and Saaltink (2020) also found that TBs located at the same site differed in the amount of precipitation measured during six rain events compared to a high-precision weighable lysimeter for bare soil conditions. The authors assumed that the TB, which showed significant errors with minor amounts of rainfall, was affected by an individual technical problem. However, the TB2 (RO; Fig. 4d) also showed a systematic underestimation of precipitation intensities, in particular for slight precipitation intensities. The TB (DD) was also prone to this circumstance and in addition showed outliers of up to 9 $mm\,h^{-1}$ during slight precipitation
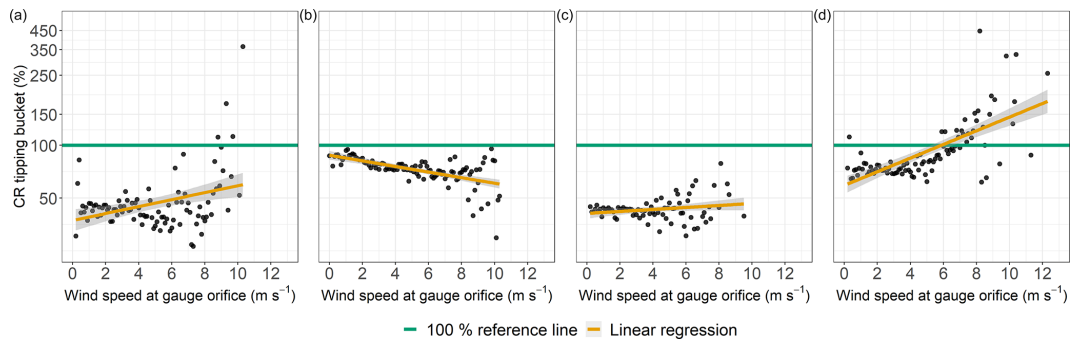
Figure 8. Catching ratios (CRs) of the tipping buckets as functions of the wind speed at gauge height for all sites, $P_{\text{ref}} \geq 0.1\,\text{mm}\,\text{h}^{-1}$, and precipitation classified as "rain". Data were binned and averaged with each bin representing a wind speed range of $0.1\,\text{m}\,\text{s}^{-1}$. **(a)** Rollesbroich lysimeter station. **(b)** Rollesbroich EC station. **(c)** Selhausen lysimeter station. **(d)** Dedelow lysimeter station.
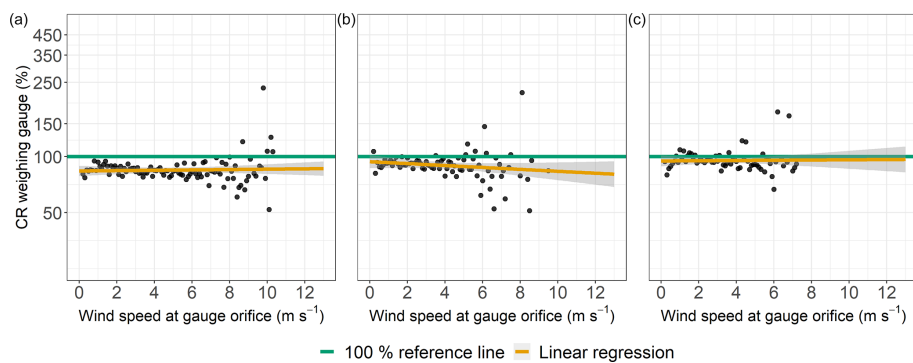

Figure 9. Catching ratios (CRs) of the weighable gauges as functions of the wind speed at gauge height, $P_{\text{ref}} \geq 0.1\,\text{mm}\,\text{h}^{-1}$, and precipitation classified as "rain". Data were binned and averaged with each bin representing a wind speed range of $0.1\,\text{m}^{-1}$. **(a)** Rollesbroich lysimeter station. **(b)** Selhausen lysimeter station before wind shield was installed. **(c)** Selhausen lysimeter station after wind shield was installed.

events. This might also be fixed with a dynamic calibration, although the occurrence of outliers towards an overestimation was exceptional compared to the other TBs. Considering that the hourly deviations led to underestimations of up to $67.7\,\%$ compared to the reference (TB RO; $n = 3483$ h), calibrations should be conducted regularly when operating a TB. TBs were also subject to the wetting loss, since precipitation can adhere to the gauge's inlet due to rough material surfaces and thus can be evaporated or sublimated without being measured (Sevruk, 1974). Due to the gauge's specific resolution, which is limited for TB gauges by the volume of a bucket, certain amounts of precipitation could not be registered and therefore got lost (loss of trace precipitation; Seibert and Morén, 1999; Sugiura et al., 2003; Yang et al., 1999b). This is particularly relevant because a minimum threshold of $0.1\,\text{mm}\,\text{h}^{-1}$ can be set for the overall comparison, but precipitation amounts below or above the gauge's resolution were not recorded by the respective TBs but only by the lysimeters. This could lead to an underestimation of precipitation amounts compared to the reference. In addition to other external influences such as wind and temperature, this is reflected in the slight systematic underestimation of the better-performing TBs.

The WGs had the best correlation with low biases and small deviations in the precipitation totals, when the internally unprocessed data were compared to the reference. At both investigation sites, the devices underestimated the precipitation intensity consistently but within or close to the uncertainty range of the reference values. The weighable gauge (WG; RO) had a slightly lower R^2 value and SDD, which might go back to generally higher wind speeds at the site. The installation of the wind shield had a positive effect on reducing the bias and SDD of the WG (SE; Fig. 5). This results agreed well with a previous study which showed that the Alter wind shield on a WG (Pluvio[2]) reduced the bias and increased the accuracy compared to an unshielded WG (Kochendorfer et al., 2017a). Overall, the WG also achieved the highest CR in the comparison of absolute precipitation at both sites. Here, too, there was a difference of $14.7\,\%$–$8.0\,\%$ compared to the reference, which could be explained by the gauge's resolution and the wind effect. These results generally support approaches from other studies (e.g., Fehlmann et al., 2020; Johannsen et al., 2020) that used the WG as a reference device to study other gauges. Although the deviations of the WG data from the lysimeter data were still rela-
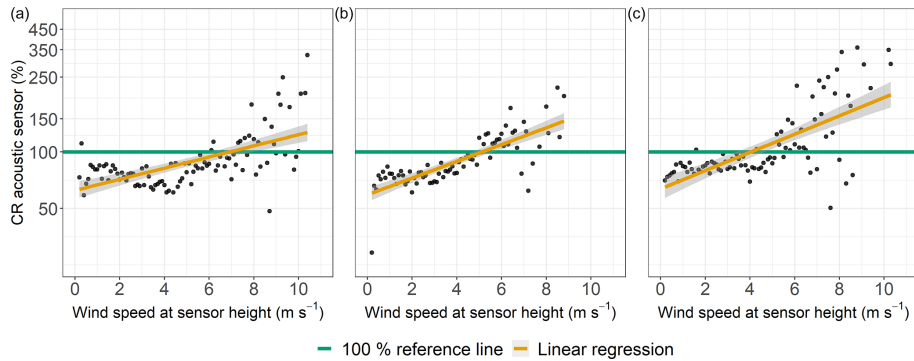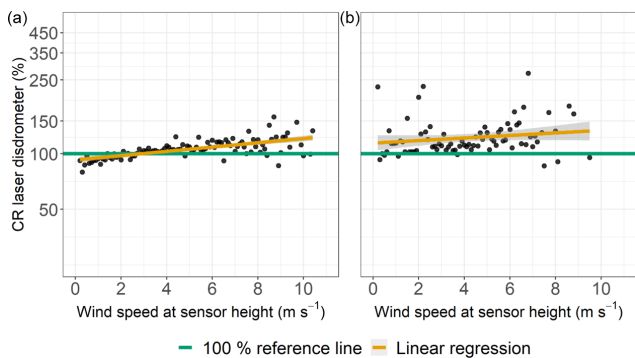
Figure 10. Catching ratios (CRs) of the acoustic sensors as functions of the wind speed at gauge height for all sites, $P_{ref} \geq 0.1\,\mathrm{mm\,h^{-1}}$, and precipitation classified as "rain". Data were binned and averaged with each bin representing a wind speed range of $0.1\,\mathrm{m\,s^{-1}}$. **(a)** Rollesbroich lysimeter station. **(b)** Selhausen lysimeter station. **(c)** Dedelow lysimeter station.

Figure 11. Catching ratios (CRs) of the laser disdrometers as functions of the wind speed at gauge height for all sites, $P_{ref} \geq 0.1\,\mathrm{mm\,h^{-1}}$, and precipitation classified as "rain". Data were binned and averaged with each bin representing a wind speed range of $0.1\,\mathrm{m\,s^{-1}}$. **(a)** Rollesbroich lysimeter station. **(b)** Selhausen lysimeter station.

tively high, this was the best correlation of all the investigated gauges in this study.

The hourly precipitation intensities determined by the AS were inaccurate compared to the reference with both over- and underestimated intensities, shown by SDDs of up to $0.7\,\mathrm{mm\,h^{-1}}$. External or internal data processing implementing an artificial time lag would lead to similarly broad scattering (Fig. 6). However the data were tested for known errors indicating a time lag, and no such influence could be identified. Salmi and Ikonen (2005) pointed out that variations in the AS measurements had more of a stochastic than a systematic origin. Variation in the shape and velocity of the hydrometeors caused by air movements was the main reason for erroneous measurements. Stochastic errors were also produced by the surface wetness and construction of the sensor itself due to sensitivity variations over the sensor area. In a comparison of multiple instruments to measure precipitation, Liu et al. (2013) found the lowest correlation coefficient and the largest SD while comparing their reference, a TB, with

the AS with a temporal resolution of 1 min. Moreover, the AS overestimated the rainfall accumulation and recorded a rain intensity that was a little higher compared to their reference when the rain intensity was less than $20\,\mathrm{mm\,h^{-1}}$ (Liu et al., 2013). According to Haselow et al. (2019), the AS showed overestimations by highly positive error values, compared to lysimeter reference data on a daily basis. Even though the hourly deviations in precipitation intensity were partly above the reference values, less absolute precipitation was measured by the ASs at all research sites than specified by the reference values. However, there were major differences between the sites. The different ASs in RO and SE registered 69.2 % and 73.2 % of the reference values, respectively, and in those DD measured 86.8 %. The variation between the sites may exist due to the selection of hours with precipitation recorded by either the TB, AS, or WG. The latter was absent in DD, so the threshold of $0.1\,\mathrm{mm\,h^{-1}}$ was more often reached by the AS at this site compared to the other sites. Therefore, precipitation registered only by the WG did not affect the CRs of the ASs at DD.

Precipitation measurements performed by the LD had a small bias compared to the reference, which was probably primarily due to the resolution of the measuring device of $0.001\,\mathrm{mm\,h^{-1}}$. The overall good correlations are reflected in the absolute values measured over a longer period, which can be compared with the CRs of the WGs. The deviations from the reference could be attributed to stochastic influences of drop size distributions and conversions during the processing of the measured data. According to a study by Johannsen et al. (2020), recorded drop sizes, velocity distributions, and kinetic energy intensity relationships were device-specific and showed similarities only for disdrometers of the same type across measurement sites. Liu et al. (2013) found that small raindrops are more likely to be overlooked in the shadow of larger raindrops. Also, two adjacent particles could appear as a large particle, resulting in wrong precipitation intensities (Lanzinger et al., 2006). The wind direction could also influence measurements of optical instruments as well
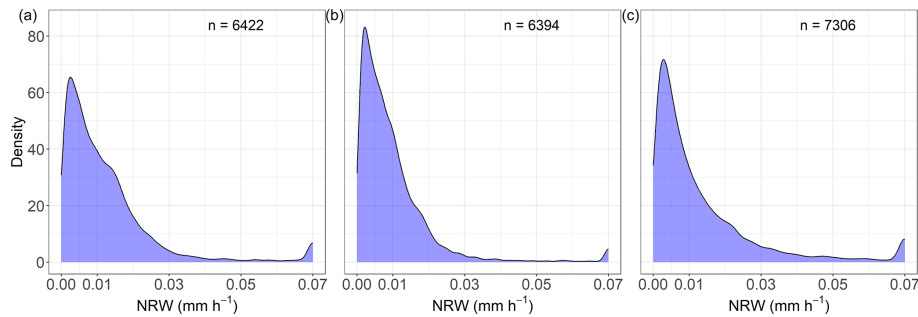
Figure 12. Distribution of non-rainfall water amounts ($P_{ref} > 0 \, \text{mm h}^{-1}$; $P_{gauge} = 0 \, \text{mm h}^{-1}$) occurring between sunset and sunrise. Hourly values of non-rainfall events were limited to a maximum value of $0.07 \, \text{mm h}^{-1}$ according to Monteith and Unsworth (2013). **(a)** Rollesbroich lysimeter station. **(b)** Selhausen lysimeter station. **(c)** Dedelow lysimeter station.

as the splashing of large raindrops off the device (Dengel et al., 2018). Hence an investigation of CRs as functions of the wind direction could reveal such interrelations. Furthermore, the number of erroneous measurements was high compared to the other gauges. For the LD (SE) 534 h must be manually filtered, compared to 42 h for the LD (RO). The data showed abrupt and isolated occurring hours with high precipitation intensities ($> 50 \, \text{mm h}^{-1}$) as well as consecutive hours with varying precipitation intensities, which were clearly decoupled from actual precipitation events. This could be explained by foreign objects interfering with the laser beam. Additionally, prolonged time periods occurred when the disdrometer continuously recorded fluctuating precipitation intensities with notable deviations from the reference. This error might be triggered by spiderwebs or insects intercepting the laser or water and dust particles on the sensor, which were known to cause such errors on optical disdrometer measurements (Adirosi et al., 2018; Heyn et al., 2018).

Ultimately, all the gauges studied tended to underestimate precipitation amounts compared to the reference, both on an hourly basis and over longer time periods. This means that calibrating large-scale weather simulations with such biased gauge data could lead to an underestimation of actual precipitation amounts in these models. The use of a less accurate precipitation dataset in environmental model calibration compromises parameter identification and reduces the ability of the model to simulate processes associated with water and solute transport in the critical zone (e.g., Groh et al., 2018a). For the calculation of small-scale water balances, biased precipitation data as an input variable could also distort the overall research results.

4.3 Influence of wind speed on gauge precipitation measurements

Of the two best-performing TBs, one (TB2, RO) exhibited generally lower CRs with increasing wind speed (Fig. 8b). This finding agreed with the general assumption of the effects of wind field formations on Hellmann design gauges

(Sevruk et al., 1989). The TB (DD) revealed increased CRs at higher wind speeds (Fig. 8d). Usually, the opposite effect is assumed (Duchon and Biddle, 2010; La Barbera et al., 2002). A connection of this phenomenon to the precipitation intensity was not evident. The AS at the site also had a higher CR than the reference at high wind speeds (Fig. 10d), but this pattern occurred also at other sites (Fig. 10b to d). The TB (DD) is the only TB installed directly within the crop field. Thus, during crop season, water from the surrounding vegetation might have dripped into the funnel and the crop might have functioned as wind protection. However, a comparison of data from the respective months with (April–July) and without available crops does not indicate such an effect.

The CRs of the WG (RO) did not indicate clear influences of wind speed on the precipitation data (Fig. 9) even though the splitting of the WG (SE) dataset according to the availability of a wind shield eventually revealed such influences affecting the measured precipitation intensities of the WGs. The CRs for the AS data imply a bias towards overestimation of precipitation intensity with increasing wind speeds. This phenomenon was recognized in the literature (Liu et al., 2013) and could be traced back to the gauge measuring principle. A wind-induced, increased terminal velocity with which a hydrometeor hits the sensors surface could be directly converted to higher precipitation intensities (Salmi and Ikonen, 2005). Both LDs tended to have increased CRs along with higher wind speeds, which might be related to the conversion from recorded drop size distribution and vertical velocity of the raindrops to precipitation intensities.

4.4 Evaluation of the precipitation data correction methods for TB and WG data

To improve data quality with precipitation data correction during post-processing, the correction method must be selected and adapted to the measuring device collecting the data (WMO, 2018). Here, two different correction methods were applied to TB and WG data to examine their impact on the respective hourly precipitation data. Both methods were based on empirical data obtained at different lo-

cations than the test sites. However, the driving forces for data correction were wind speed and gauge design, which in this study were similar to those of the original data correction studies. Both approaches reduced the bias of the TB data relative to the reference, which was a key goal of the precipitation data correction. The dynamic correction model (DCM) led to a generally greater reduction in the bias (TBs: $-0.13\,\mathrm{mm\,h^{-1}}$; WGs: $-0.09\,\mathrm{mm\,h^{-1}}$) for all gauges than the approach derived from the method of Richter (1995; TBs: $-0.08\,\mathrm{mm\,h^{-1}}$; WGs: $-0.07\,\mathrm{mm\,h^{-1}}$). As a result of the corrections, considerable amounts of precipitation have been added to the precipitation totals in the period under study. In particular, the correction of data from TB2 (RO), WG (RO), and WG (SE) led to CRs of 97.4 % (+15.7 %), 96.0 % (+10.7 %), and 100.5 % (+8.5 %) compared to the lysimeter reference. This indicates that the correction methods showed the best effect for the data with the initially highest quality but could possibly lead to overestimations, which was found in overcorrection of precipitation data for WG (Se; Table 7).

Haselow et al. (2019) used the linear scaling method to reduce the bias of daily precipitation data from multiple rain gauges compared to lysimeter measurements. To do this, they applied the ratio of the monthly rainfall totals from lysimeters and rain gauges to the daily rainfall totals of the rain gauges. The method successfully reduced the bias of the daily precipitation data despite periods of high precipitation intensities (Haselow et al., 2019). However, a distinction must be made between correction methods that correct precipitation data solely on the basis of reference data (e.g., Fang et al., 2015) and methods such as the DCM used in this study that correct individual physically and technically induced errors like wind field deformation and evaporation. For the latter approach, the availability of results from comparable studies with weighable lysimeter references is limited. For TB1 (RO) and TB (SE), the correction was not sufficient to compensate for the systematic biases from the reference, although the distortion probably came from calibration issues that were not intended to be corrected by the DCM. An overcorrection of the precipitation intensities for the WGs at high wind speeds cannot be ruled out, especially since the Alter wind shield has already reduced the influence of the wind on the WG (SE). Michelson (2004) found that the DCM resulted in more accurate precipitation estimates, although uncertainties in the treatment of measurements for some gauge types remain, which can be confirmed by the results of this work. The results also showed that the biases for all corrected TBs were reduced by applying the adjusted correction method according to Richter (1995), although high biases still remain for the TB1 (RO), TB (SE), and TB (DD). It must be taken into account that the orders of magnitude of these correction amounts were detached from individual environmental influences at the sites and only related to the manual Hellmann-type gauge (Richter, 1995). Richter (1995) also stated that due to the large daily variability in the individual error-causing parameters, the statistical error in the calculations based on mean ratios was inevitably large and mainly of the magnitude of the correction amount. Therefore, the adjustment to correct the hourly measurements increased the statistical error. Based on the given data availability of reference, gauge, and weather data, machine learning algorithms might be a promising tool to further optimize device-specific precipitation data corrections.

5 Conclusions

Precipitation data from three research sites of the TERENO-SOILCan network based on high-precision weighable lysimeters were used as a reference to investigate the functionality and data quality of four different precipitation measurement methods. The low bias in hourly lysimeter measurements indicated the suitability of their arithmetic mean as a reference for comparing precipitation methods. The results of this study revealed that each gauge-based method (i.e., tipping bucket gauges, weighable gauges, acoustic sensors, and optical laser disdrometers) was affected differently by wind, precipitation intensity, measurement resolution, and technical errors. All precipitation measurement methods underestimated the precipitation amounts for the observation period with deviations of 8 % to 67 % from the reference if only hours with precipitation intensities greater than $0.1\,\mathrm{mm\,h^{-1}}$ were considered. This implies that point precipitation data should be treated as minimum values, especially when looking at cumulative totals over long time periods. When using hourly data for water balances or local projections of climate change, an uncertainty regarding over- and underestimation of point precipitation data must be taken into account, depending on the gauge type. The results confirmed that correction algorithms, which consider the influence of wind and other typical sources of error on the instruments, reduced the bias between reference and measurements and improved the catching ratios of hourly precipitation data from rain gauges (tipping bucket and weighable gauge) under different climatic conditions at three different TERENO-SOILCan test sites. The dynamic correction model achieved higher average catch ratios compared to the correction approach derived from Richter. Therefore, only the dynamic correction model might be the right tool to correct hourly precipitation data. Adequate reference data are crucial for testing and developing correction methods to overcome errors in precipitation measurements from standard point gauges. Observations from weighable, high-precision lysimeters (e.g., the TERENO-SOILCan network) provide such data to improve estimates of point-scale precipitation under different climatic conditions. Unbiased point-scale precipitation estimates are essential when estimating precipitation at larger scales remotely from either ground-based weather radars or from satellites. Precipitation is the main driver of the hydrological cycle, and accurate data help to improve local weather

and climate forecasts, which is particularly relevant in the context of climate change.
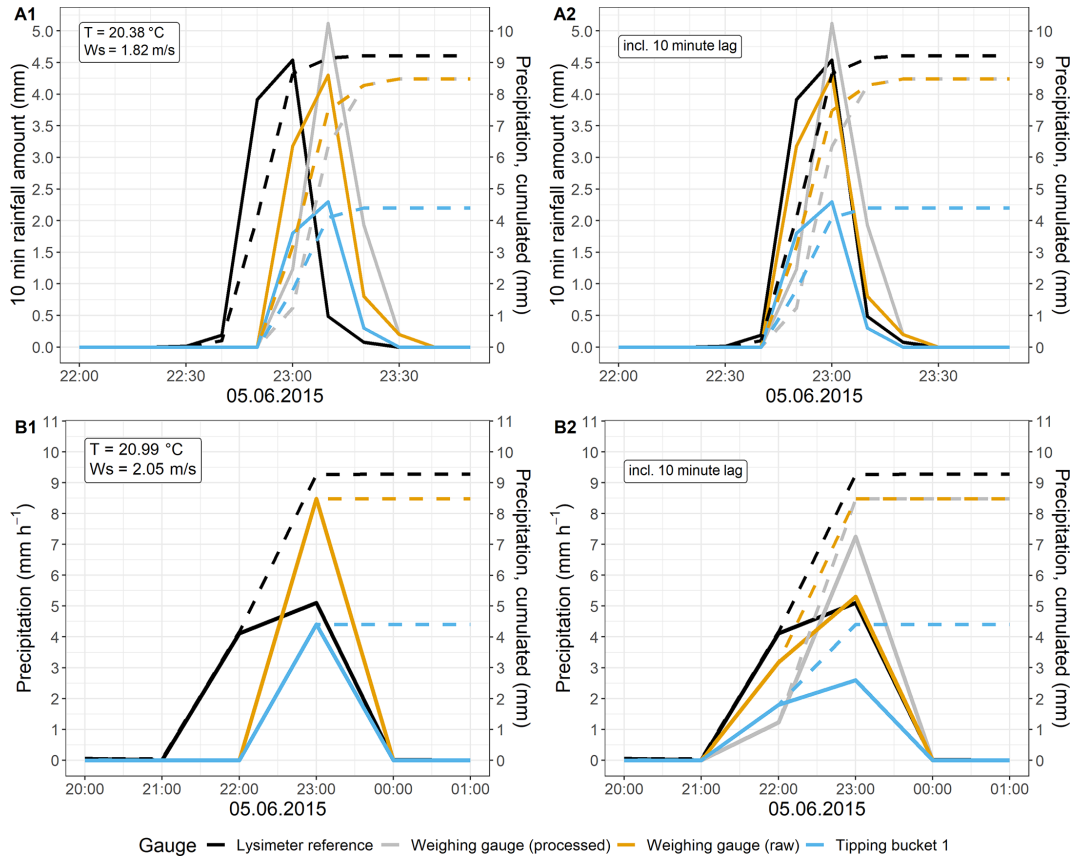
Appendix A

Figure A1. Time series of a precipitation event in Selhausen with a temporal resolution of **(a)** 10 min and **(b)** 1 h. Solid lines display the precipitation intensity (left y axis) and dashed lines the cumulative precipitation (right y axis). **(A1)** and **(B1)** show original data. **(A2)** and **(B2)** show data with an implemented reverse time lag of 10 min for the tipping bucket and weighable gauge.

Appendix B

Table B1. Distribution of precipitation rates determined by the lysimeters over the observation period for $P_{\text{ref}} \geq 0.1 \ \mathrm{mm\,h^{-1}}$, as used for the gauge comparison.

Site	Min	Max	Mean	Median	Quantiles ($\mathrm{mm\,h^{-1}}$)				
	($\mathrm{mm\,h^{-1}}$)	($\mathrm{mm\,h^{-1}}$)	($\mathrm{mm\,h^{-1}}$)	($\mathrm{mm\,h^{-1}}$)	5.00 %	25.00 %	50.00 %	75.00 %	95.0,%
Rollesbroich	0.100	32.243	0.822	0.413	0.114	0.202	0.413	0.885	2.813
Selhausen	0.100	23.210	0.941	0.519	0.120	0.248	0.519	1.145	2.941
Dedelow	0.100	12.910	0.819	0.446	0.116	0.209	0.446	0.973	2.626

Table B2. Distribution of precipitation rates determined by the lysimeters over the observation period for $P_{\text{ref}} > 0\,\text{mm}\,\text{h}^{-1}$, including non-rainfall water.

Site	Min	Max	Mean	Median	Quantiles ($\text{mm}\,\text{h}^{-1}$)				
	($\text{mm}\,\text{h}^{-1}$)	($\text{mm}\,\text{h}^{-1}$)	($\text{mm}\,\text{h}^{-1}$)	($\text{mm}\,\text{h}^{-1}$)	5.00 %	25.00 %	50.00 %	75.00 %	95.00 %
Rollesbroich	0.001	32.243	0.177	0.013	0.001	0.005	0.013	0.052	0.883
Selhausen	0.001	23.210	0.297	0.017	0.001	0.006	0.017	0.195	1.536
Dedelow	0.001	12.910	0.220	0.014	0.001	0.005	0.014	0.106	1.189

Appendix C
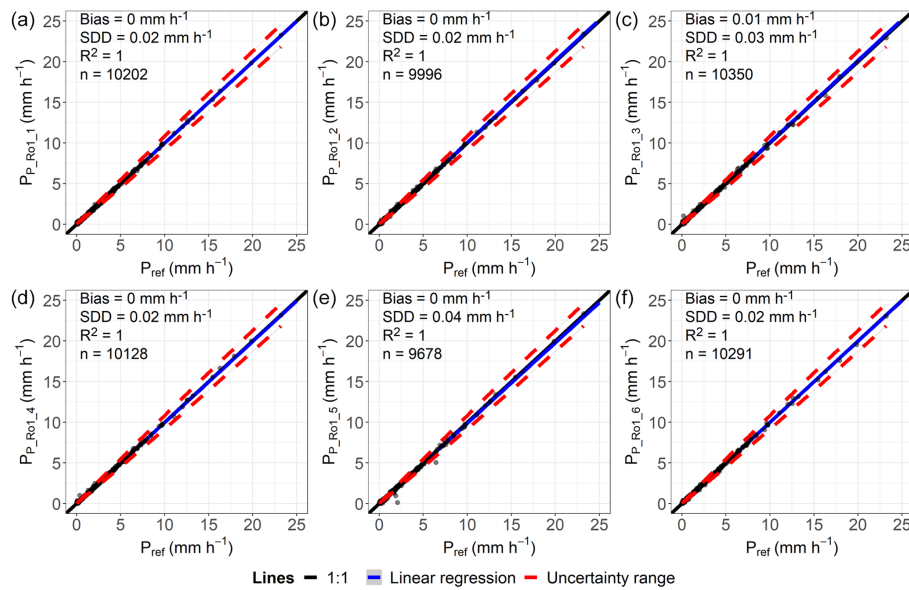
Figure C1. Comparison of hourly precipitation data classified as "rain", determined by lysimeter and reference data (P_{ref}) for the lysimeter station in Rollesbroich. Plots **(a)**–**(f)** include all hours of measurements taken where both P_{lys} and P_{ref} are $\geq 0.001\,\text{mm}\,\text{h}^{-1}$. The vegetation grown on the lysimeter is of a grassland type.
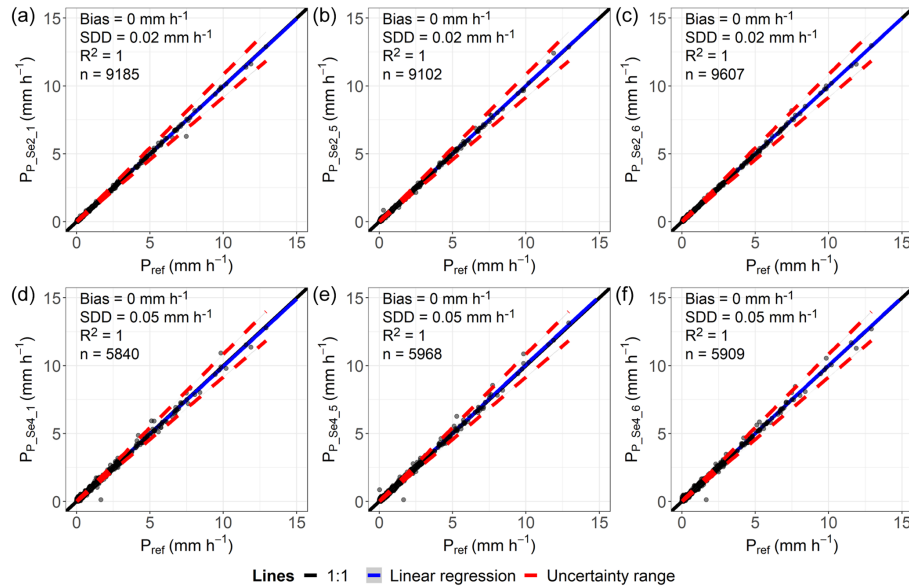
Figure C2. Comparison of hourly precipitation data classified as "rain", determined by lysimeter and reference data (P_{ref}) for the lysimeter station in Selhausen. Plots **(a)**–**(c)** include all hours of measurements taken where both P_{lys} and P_{ref} are $\geq 0.001\,\text{mm}\,\text{h}^{-1}$ and the vegetation grown on the lysimeter is of a grassland type. Plots **(d)**–**(f)** include all hours of measurements taken where both P_{lys} and P_{ref} are $\geq 0.001\,\text{mm}\,\text{h}^{-1}$ and the vegetation grown on the lysimeter is of an arable land type.
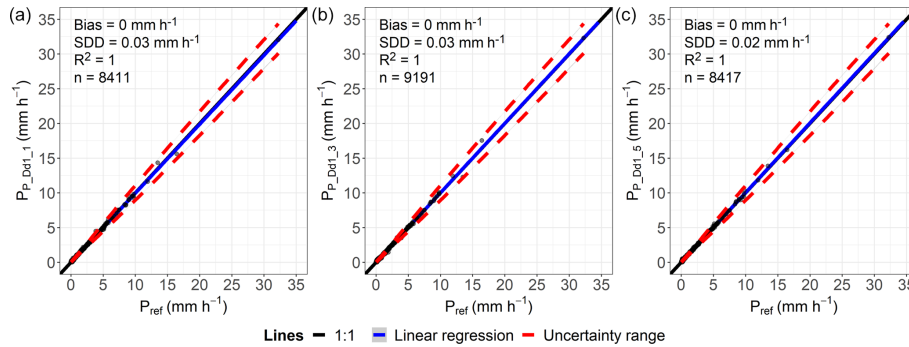
Figure C3. Comparison of hourly precipitation data classified as "rain", determined by lysimeter and reference data (P_{ref}) for the lysimeter station in Dedelow. Plots **(a)**–**(c)** include all hours of measurements taken where both P_{lys} and P_{ref} are $\geq 0.001\,\text{mm}\,\text{h}^{-1}$. The vegetation grown on the lysimeter is of an arable land type.

Appendix D

Table D1. Mean and variance for all measurements taken by the lysimeter at each site for hours in which every lysimeter at a site has been available during the investigation period (2015–2018). Data filtered for "rain" and $P > 0.1\,\mathrm{mm\,h^{-1}}$.

	Lysimeter	Rollesbroich	Selhausen	Dedelow
Mean	1	0.887	0.824	0.815
$(\mathrm{mm\,h^{-1}})$	2	0.901	0.826	0.823
	3	0.907	0.824	0.829
	4	0.884	0.822	
	5	0.877	0.826	
	6	0.893	0.828	
Variance	1	1.67	1.27	1.93
$(\mathrm{mm\,h^{-1}})^2$	2	1.69	1.28	1.96
	3	1.69	1.28	1.97
	4	1.67	1.27	
	5	1.64	1.30	
	6	1.66	1.28	

Appendix E

Table E1. Statistics on non-rainfall water (NRW) recorded by the lysimeter within the investigated period. NRW was identified when no gauge but the lysimeter or disdrometer recorded atmospheric water input (AWI) between sunrise and sunset. The statistics are given for $\mathrm{NRW} \le 0.07\,\mathrm{mm\,h^{-1}}$.

Site (–)	Year (–)	Sum $(\mathrm{mm\,h^{-1}})$	Mean $(\mathrm{mm\,h^{-1}})$	Median $(\mathrm{mm\,h^{-1}})$	Standard deviation $(\mathrm{mm\,h^{-1}})$	n (h)	n (NRW $> 0.07\,\mathrm{mm\,h^{-1}}$) (h)
Rollesbroich	2015	14.3	0.012	0.010	0.010	1245	18
	2016	20.1	0.011	0.008	0.011	1807	53
	2017	18.7	0.012	0.009	0.011	1585	46
	2018	16.1	0.010	0.007	0.009	1639	29
Selhausen	2015	15.8	0.011	0.008	0.010	1505	22
	2016	14.1	0.009	0.006	0.008	1636	16
	2017	14.3	0.009	0.007	0.009	1544	19
	2018	12.9	0.008	0.006	0.007	1636	16
Dedelow	2015	22.0	0.012	0.009	0.011	1767	40
	2016	24.0	0.012	0.007	0.013	1944	63
	2017	20.4	0.013	0.009	0.013	1532	61
	2018	16.3	0.009	0.005	0.010	1838	61

References

Adirosi, E., Roberto, N., Montopoli, M., Gorgucci, E., and Baldini, L.: Influence of Disdrometer Type on Weather Radar Algorithms from Measured DSD: Application to Italian Climatology, Atmosphere, 9, 360, https://doi.org/10.3390/atmos9090360, 2018.

Alter, J. C.: Shielded storage precipitation gages, Mon. Weather Rev., 65, 262–265, https://doi.org/10.1175/1520-0493(1937)65<262:SSPG>2.0.CO;2, 1937.

Bárdossy, A., Kilsby, C., Birkinshaw, S., Wang, N., and Anwar, F.: Is Precipitation Responsible for the Most Hydrological Model Uncertainty?, Front. Water, 4, 836554, https://doi.org/10.3389/frwa.2022.836554, 2022.

Bloemink, H. I. and Lanzinger, E.: Precipitation type from the Thies disdrometer, WMO, Bukarest, https://cdn.knmi.nl/system/data_center_publications/files/000/068/578/original/teco2005_paper_bloemink.pdf?1495621277 (last access: 1 September 2022), 2005.

Bogena, H. R., Montzka, C., Huisman, J. A., Graf, A., Schmidt, M., Stockinger, M., von Hebel, C., Hendricks-Franssen, H. J., van der Kruk, J., Tappe, W., Lücke, A., Baatz, R., Bol, R., Groh, J., Pütz, T., Jakobi, J., Kunkel, R., Sorg, J., and Vereecken, H.: The TERENO-Rur Hydrological Observatory: A Multi-scale Multi-Compartment Research Platform for the Advancement of Hydrological Science, Vadose Zone J., 17, 180055, https://doi.org/10.2136/vzj2018.03.0055, 2018.

Calder, I. R. and Kidd, C.: A note on the dynamic calibration of tipping-bucket gauges, J. Hydrol., 39, 383–386, https://doi.org/10.1016/0022-1694(78)90013-6, 1978.

Chen, R., Liu, J., Kang, E., Yang, Y., Han, C., Liu, Z., Song, Y., Qing, W., and Zhu, P.: Precipitation measurement intercomparison in the Qilian Mountains, north-eastern Tibetan Plateau, The Cryosphere, 9, 1995–2008, https://doi.org/10.5194/tc-9-1995-2015, 2015.

Chvíla, B., Sevruk, B., and Ondrás, M.: The wind-induced loss of thunderstorm precipitation measurements, Atmos. Res., 77, 29–38, https://doi.org/10.1016/j.atmosres.2004.11.032, 2005.

Dengel, S., Graf, A., Grünwald, T., Hehn, M., Kolari, P., Löfvenius, M. O., Merbold, L., Nicolini, G., and Pavelka, M.: Standardized precipitation measurements within ICOS: rain, snowfall and snow depth: a review, Int. Agrophys., 32, 607–617, https://doi.org/10.1515/intag-2017-0046, 2018.

Duchon, C. E. and Biddle, C. J.: Undercatch of tipping-bucket gauges in high rain rate events, Adv. Geosci., 25, 11–15, https://doi.org/10.5194/adgeo-25-11-2010, 2010.

Duchon, C. E. and Essenberg, G. R.: Comparative rainfall observations from pit and aboveground rain gauges with and without wind shields, Water Resour. Res., 37, 3253–3263, https://doi.org/10.1029/2001WR000541, 2001.

DWD: Niederschlag: vieljährige Mittelwerte 1961–1990, Deutscher Wetterdienst, https://www.dwd.de/DE/leistungen/klimadatendeutschland/mittelwerte/nieder_6190_akt_html.html?view=nasPublication&nn=16102 (last access: 8 October 2021), 2021a.

DWD: Temperatur: vieljährige Mittelwerte 1961–1990, Deutscher Wetterdienst, https://www.dwd.de/DE/leistungen/klimadatendeutschland/mittelwerte/temp_6190_akt_html.html?view=nasPublication&nn=16102 (last access: 8 October 2021), 2021b.

Fang, G. H., Yang, J., Chen, Y. N., and Zammit, C.: Comparing bias correction methods in downscaling meteorological variables for a hydrologic impact study in an arid area in China, Hydrol. Earth Syst. Sci., 19, 2547–2559, https://doi.org/10.5194/hess-19-2547-2015, 2015.

Fehlmann, M., Rohrer, M., von Lerber, A., and Stoffel, M.: Automated precipitation monitoring with the Thies disdrometer: biases and ways for improvement, Atmos. Meas. Tech., 13, 4683–4698, https://doi.org/10.5194/amt-13-4683-2020, 2020.

Førland, E. J., Allerup, P., Dahlström, B., Elomaa, E., Jónsson, T., Madsen, H., Perälä, J., Rissanen, P., Vedin, H., and Vejen, F.: Manual for Operational Correction of Nordic Precipitation Data, Oslo, https://www.met.no/publikasjoner/met-report/met-report-1996/_/attachment/download/ea2cb006-688a-408f-a60c-9f6306843cc0:e16a138129a1d1896cff764ab3eb2cc42aefb160/MET-report-24-1996.pdf (last access: 1 May 2022), 1996.

Forstner, V., Groh, J., Vremec, M., Herndl, M., Vereecken, H., Gerke, H. H., Birk, S., and Pütz, T.: Response of water fluxes and biomass production to climate change in permanent grassland soil ecosystems, Hydrol. Earth Syst. Sci., 25, 6087–6106, https://doi.org/10.5194/hess-25-6087-2021, 2021.

Fuchs, T., Rapp, J., Rubel, F., and Rudolf, B.: Correction of synoptic precipitation observations due to systematic measuring errors with special regard to precipitation phases, Phys. Chem. Earth Pt. B, 26, 689–693, https://doi.org/10.1016/S1464-1909(01)00070-3, 2001.

Gebler, S., Hendricks Franssen, H.-J., Pütz, T., Post, H., Schmidt, M., and Vereecken, H.: Actual evapotranspiration and precipitation measured by lysimeters: a comparison with eddy covariance and tipping bucket, Hydrol. Earth Syst. Sci., 19, 2145–2161, https://doi.org/10.5194/hess-19-2145-2015, 2015.

Gebler, S., Hendricks Franssen, H.-J., Kollet, S. J., Qu, W., and Vereecken, H.: High resolution modelling of soil moisture patterns with TerrSysMP: A comparison with sensor network data, J. Hydrol., 547, 309–331, https://doi.org/10.1016/j.jhydrol.2017.01.048, 2017.

Goodison, B. E., Louie, P., and Yang, D.: WMO Solid Precipitation Measurement Intercomparison, Final Report, Instruments and observing methods, World Meteorological Organization, 67 pp. https://library.wmo.int/index.php?lvl=notice_display&id=6441 (last access: 1 September 2022), 1998.

Goss, M. J. and Ehlers, W.: The role of lysimeters in the development of our understanding of soil water and nutrient dynamics in ecosystems, Soil Use Manage., 25, 213–223, https://doi.org/10.1111/j.1475-2743.2009.00230.x, 2009.

Groh, J., Stumpp, C., Lücke, A., Pütz, T., Vanderborght, J., and Vereecken, H.: Inverse Estimation of Soil Hydraulic and Transport Parameters of Layered Soils from Water Stable Isotope and Lysimeter Data, Vadose Zone J., 17, 170168, https://doi.org/10.2136/vzj2017.09.0168, 2018a.

Groh, J., Slawitsch, V., Herndl, M., Graf, A., Vereecken, H., and Pütz, T.: Determining dew and hoar frost formation for a low mountain range and alpine grassland site by weighable lysimeter, J. Hydrol., 563, 372–381, https://doi.org/10.1016/j.jhydrol.2018.06.009, 2018b.

Groh, J., Pütz, T., Gerke, H. H., Vanderborght, J., and Vereecken, H.: Quantification and Prediction of Nighttime Evapotranspiration for Two Distinct Grassland Ecosystems, Water Resour. Res., 55, 2961–2975, https://doi.org/10.1029/2018WR024072, 2019.

Groh, J., Diamantopoulos, E., Duan, X., Ewert, F., Herbst, M., Holbak, M., Kamali, B., Kersebaum, K.-C., Kuhnert, M., Lischeid, G., Nendel, C., Priesack, E., Steidl, J., Sommer, M., Pütz, T., Vereecken, H., Wallor, E., Weber, T. K., Wegehenkel, M., Weihermüller, L., and Gerke, H. H.: Crop growth and soil water fluxes at erosion-affected arable sites: Using weighing lysimeter data for model intercomparison, Vadose Zone J., 19, e20058, https://doi.org/10.1002/vzj2.20058, 2020a.

Groh, J., Vanderborght, J., Pütz, T., Vogel, H.-J., Gründling, R., Rupp, H., Rahmati, M., Sommer, M., Vereecken, H., and Gerke, H. H.: Responses of soil water storage and crop water use efficiency to changing climatic conditions: a lysimeter-based space-for-time approach, Hydrol. Earth Syst. Sci., 24, 1211–1225, https://doi.org/10.5194/hess-24-1211-2020, 2020b.

Hagenau, J., Meissner, R., and Borg, H.: Effect of exposure on the water balance of two identical lysimeters, J. Hydrol., 520, 69–74, https://doi.org/10.1016/j.jhydrol.2014.11.030, 2015.

Hannes, M., Wollschläger, U., Schrader, F., Durner, W., Gebler, S., Pütz, T., Fank, J., von Unold, G., and Vogel, H.-J.: A comprehensive filtering scheme for high-resolution estimation of the water balance components from high-precision lysimeters, Hydrol. Earth Syst. Sci., 19, 3405–3418, https://doi.org/10.5194/hess-19-3405-2015, 2015.

Haselow, L., Meissner, R., Rupp, H., and Miegel, K.: Evaluation of precipitation measurements methods under field conditions during a summer season: A comparison of the standard rain gauge with a weighable lysimeter and a piezoelectric precipitation sensor, J. Hydrol., 575, 537–543, https://doi.org/10.1016/j.jhydrol.2019.05.065, 2019.

Heinrich, I., Balanzategui, D., Bens, O., Blasch, G., Blume, T., Böttcher, F., Borg, E., Brademann, B., Brauer, A., Conrad, C., Dietze, E., Dräger, N., Fiener, P., Gerke, H. H., Güntner, A., Heine, I., Helle, G., Herbrich, M., Harfenmeister, K., Heußner, K.-U., Hohmann, C., Itzerott, S., Jurasinski, G., Kaiser, K., Kappler, C., Koebsch, F., Liebner, S., Lischeid, G., Merz, B., Missling, K. D., Morgner, M., Pinkerneil, S., Plessen, B., Raab, T., Ruhtz, T., Sachs, T., Sommer, M., Spengler, D., Stender, V., Stüve, P., and Wilken, F.: Interdisciplinary Geo-ecological Research across Time Scales in the Northeast German Lowland Observatory (TERENO-NE), Vadose Zone J., 17, 180116, https://doi.org/10.2136/vzj2018.06.0116, 2018.

Herbrich, M. and Gerke, H. H.: Autocorrelation analysis of high resolution weighing lysimeter time series as a basis for determination of precipitation, Z. Pflanzenernähr. Bodenk., 179, 784–798, https://doi.org/10.1002/jpln.201600169, 2016.

Hertel, C. and von Unold, G.: Third-generation lysimeters: scientific engineered monitoring systems, in: Novel measurement and assessment tools for monitoring and management of land and water resources in agricultural landscapes of central Asia, edited by: Mueller, L., Saparov, A., and Lischeid, G., Springer International Cham, Heidelberg, New York, Dordrecht, London, 175–184, https://doi.org/10.1007/978-3-319-01017-5_9, 2013.

Heyn, K., Lönnqvist, J., and Linna, T.: Uncertainty sources that limit the precipitation identification / quantification ad extinction coefficient determination capabilities of optical present weather and visibility sensors, in: WMO Technical Conference on Meteorological and Environmental Instruments

and Methods of Observation, 8–11 October 2018, Amsterdam, the Netherlands, https://www.wmocimo.net/wp-content/uploads/O2_13_Heyn_TECO-2018-K.Heyn-O2-13.pdf (last access: 1 September 2022), 2018.

Hoffmann, M., Schwartengräber, R., Wessolek, G., and Peters, A.: Comparison of simple rain gauge measurements with precision lysimeter data, Atmos. Res., 174–175, 120–123, https://doi.org/10.1016/j.atmosres.2016.01.016, 2016.

Johannsen, L. L., Zambon, N., Strauss, P., Dostal, T., Neumann, M., Zumr, D., Cochrane, T. A., Blöschl, G., and Klik, A.: Comparison of three types of laser optical disdrometers under natural rainfall conditions, Hydrolog. Sci. J., 65, 524–535, https://doi.org/10.1080/02626667.2019.1709641, 2020.

Kochendorfer, J., Nitu, R., Wolff, M., Mekis, E., Rasmussen, R., Baker, B., Earle, M. E., Reverdin, A., Wong, K., Smith, C. D., Yang, D., Roulet, Y.-A., Buisan, S., Laine, T., Lee, G., Aceituno, J. L. C., Alastrué, J., Isaksen, K., Meyers, T., Brækkan, R., Landolt, S., Jachcik, A., and Poikonen, A.: Analysis of single-Alter-shielded and unshielded measurements of mixed and solid precipitation from WMO-SPICE, Hydrol. Earth Syst. Sci., 21, 3525–3542, https://doi.org/10.5194/hess-21-3525-2017, 2017a.

Kochendorfer, J., Rasmussen, R., Wolff, M., Baker, B., Hall, M. E., Meyers, T., Landolt, S., Jachcik, A., Isaksen, K., Brækkan, R., and Leeper, R.: The quantification and correction of wind-induced precipitation measurement errors, Hydrol. Earth Syst. Sci., 21, 1973–1989, https://doi.org/10.5194/hess-21-1973-2017, 2017b.

Kohfahl, C. and Saaltink, M. W.: Comparing precision lysimeter rainfall measurements against rain gauges in a coastal dune belt, Spain, J. Hydrol., 591, 125580, https://doi.org/10.1016/j.jhydrol.2020.125580, 2020.

Kunkel, R., Sorg, J., Klump, J., Kolditz, O., Rink, K., Gasche, R., and Neidl, F.: TEODOOR - A Spatial Data Infrastructure for terrestrial observation data, in: 2013 10th IEEE International Conference on Networking, Sensing and Control (IC-NSC 2013): Evry, Evry, France, 10–12 April 2013, 242–245, https://doi.org/10.1109/ICNSC.2013.6548744, 2013.

La Barbera, P., Lanza, L. G., and Stagi, L.: Tipping bucket mechanical errors and theirs influence on rainfall statistics and extremes, Water Sci. Technol., 45, 1–9, https://doi.org/10.2166/wst.2002.0020, 2002.

Lanza, L. G. and Vuerich, E.: The WMO Field Intercomparison of Rain Intensity Gauges, Atmos. Res., 94, 534–543, https://doi.org/10.1016/j.atmosres.2009.06.012, 2009.

Lanzinger, E., Theel, M., and Windolph, H.: Rainfall Amount and Intensity measured by the Thies Laser Precipitation Monitor, TECO-2006, Geneva, Switzerland, https://api.semanticscholar.org/CorpusID:898320 (last access: 1 September 2022), 2006.

Liu, X. C., Gao, T. C., and Liu, L.: A comparison of rainfall measurements from multiple instruments, Atmos. Meas. Tech., 6, 1585–1595, https://doi.org/10.5194/amt-6-1585-2013, 2013.

Marek, G., Evett, S., Gowda, P. H., Howell, T. A., Copeland, K. S., and Baumhardt, R. L.: Post-Processing Techniques for Reducing Errors in Weighing Lysimeter Evapotranspiration (ET) Datasets, T. ASABE, 499–515, https://doi.org/10.13031/trans.57.10433, 2014.

McGuiness, J. L.: A comparison of lysimeter catch and rain gage catch, Agricultural Research Service, 124 pp. ARS 41-124, 1966.

Meissner, R., Seeger, J., Rupp, H., Seyfarth, M., and Borg, H.: Measurement of dew, fog, and rime with a high-precision gravitation lysimeter, Z. Pflanzenernähr. Bodenk., 170, 335–344, https://doi.org/10.1002/jpln.200625002, 2007.

Michaelides, S., Levizzani, V., Anagnostou, E., Bauer, P., Kasparis, T., and Lane, J. E.: Precipitation: Measurement, remote sensing, climatology and modeling, Atmos. Res., 94, 512–533, https://doi.org/10.1016/j.atmosres.2009.08.017, 2009.

Michelson, D. B.: Systematic correction of precipitation gauge observations using analyzed meteorological variables, J. Hydrol., 290, 161–177, https://doi.org/10.1016/j.jhydrol.2003.10.005, 2004.

Monteith, J. L. and Unsworth, M. H.: Principles of environmental physics: Plants, animals, and the atmosphere, in: 4th Edn., Elsevier/Acad. Press, Amsterdam, 401 pp., ISBN 978-0-12-386910-4, 2013.

Morgan, D. L. and Lourence, F. J.: Comparison Between Rain Gage and Lysimeter Measurements, Water Resour. Res., 5, 724–728, https://doi.org/10.1029/WR005i003p00724, 1969.

Niemczynowicz, J.: The Dynamic Calibration of Tipping-Bucket Raingauges, Hydrol. Res., 17, 203–214, https://doi.org/10.2166/nh.1986.0013, 1986.

Nipher, F. E.: On the determination of the true rainfall, by elevated gages, in: Proceedings of the American Association for the Advancement of Science, August 1878, St. Louis, Missouri, USA, 103–108, 1878.

Nolz, R., Kammerer, G., and Cepuder, P.: Interpretation of lysimeter weighing data affected by wind, Z. Pflanzenernähr. Bodenk., 176, 200–208, https://doi.org/10.1002/jpln.201200342, 2013.

Peters, A., Nehls, T., Schonsky, H., and Wessolek, G.: Separating precipitation and evapotranspiration from noise – a new filter routine for high-resolution lysimeter data, Hydrol. Earth Syst. Sci., 18, 1189–1198, https://doi.org/10.5194/hess-18-1189-2014, 2014.

Peters, A., Nehls, T., and Wessolek, G.: Technical note: Improving the AWAT filter with interpolation schemes for advanced processing of high resolution data, Hydrol. Earth Syst. Sci., 20, 2309–2315, https://doi.org/10.5194/hess-20-2309-2016, 2016.

Peters, A., Groh, J., Schrader, F., Durner, W., Vereecken, H., and Pütz, T.: Towards an unbiased filter routine to determine precipitation and evapotranspiration from high precision lysimeter measurements, J. Hydrol., 549, 731–740, https://doi.org/10.1016/j.jhydrol.2017.04.015, 2017.

Pollock, M. D., O'Donnell, G., Quinn, P., Dutton, M., Black, A., Wilkinson, M. E., Colli, M., Stagnaro, M., Lanza, L. G., Lewis, E., Kilsby, C. G., and O'Connell, P. E.: Quantifying and Mitigating Wind-Induced Undercatch in Rainfall Measurements, Water Resour. Res., 54, 3863–3875, https://doi.org/10.1029/2017WR022421, 2018.

Porporato, A. and Rodriguez-Iturbe, I.: Ecohydrology – a challenging multidisciplinary research perspective, Hydrolog. Sci. J., 47, 811–821, https://doi.org/10.1080/02626660209492985, 2002.

Pütz, T., Kiese, R., Wollschläger, U., Groh, J., Rupp, H., Zacharias, S., Priesack, E., Gerke, H. H., Gasche, R., Bens, O., Borg, E., Baessler, C., Kaiser, K., Herbrich, M., Munch, J.-C., Sommer, M., Vogel, H.-J., Vanderborght, J., and Vereecken, H.: TERENO-SOILCan: a lysimeter-network in Germany observing soil processes and plant diversity influenced by climate change, Environ.

Earth Sci., 75, 1242, https://doi.org/10.1007/s12665-016-6031-5, 2016.

R Core Team: R: A language and environment for statistical computing, R Foundation for Statistical Computing, Vienna, Austria, https://www.r-project.org/ (last access: 1 September 2022), 2020.

Richter, D.: Ergebnisse methodischer Untersuchungen zur Korrektur des systematischen Meßfehlers des Hellmann-Niederschlagmessers, Berichte des Deutschen Wetterdienstes, Selbstverlag des Deutschen Wetterdienstes, Offenbach am Main, 194 pp. ISBN 9783881483094, 1995.

Ross, A., Smith, C. D., and Barr, A.: An improved post-processing technique for automatic precipitation gauge time series, Atmos. Meas. Tech., 13, 2979–2994, https://doi.org/10.5194/amt-13-2979-2020, 2020.

Ryu, S., Lee, G., Nitu, R., Smith, C., Lim, E., and Kim, H. L.: Quantitative comparison of two types of working field reference systems for the measurement of precipitation amount (R^2), in: Proceedings of the WMO Technical Conference on Meteorological and Environmental Instruments and Methods of Observation, September 2016, Madrid, Spain, 2016.

Salmi, A. and Ikonen, J.: Piezoelectric precipitation sensor from Vaisala, in: WMO Technical Conference on Instruments and Methods of Observation (TECO-2005), https://library.wmo.int/index.php?lvl=notice_display&id=11280 (last access: 1 September 2022), Bucharest, Romania, 4–7 May 2005, 2005.

Schneider, J., Groh, J., Pütz, T., Helmig, R., Rothfuss, Y., Vereecken, H., and Vanderborght, J.: Prediction of soil evaporation measured with weighable lysimeters using the FAO Penman–Monteith method in combination with Richards' equation, Vadose Zone J., 20, 1, https://doi.org/10.1002/vzj2.20102, 2021.

Schrader, F., Durner, W., Fank, J., Gebler, S., Pütz, T., Hannes, M., and Wollschläger, U.: Estimating Precipitation and Actual Evapotranspiration from Precision Lysimeter Measurements, Proced. Environ. Sci., 19, 543–552, https://doi.org/10.1016/j.proenv.2013.06.061, 2013.

Seibert, J. and Morén, A.-S.: Reducing systematic errors in rainfall measurements using a new type of gauge, Agr. Forest Meteorol., 98–99, 341–348, https://doi.org/10.1016/S0168-1923(99)00107-0, 1999.

Sevruk, B.: Correction for the wetting loss of a Hellmann precipitation gauge, Hydrolog. Sci. Bull., 194, 549–559, 1974.

Sevruk, B.: Methods of correction for systematic error in point precipitation measurement for operational use, Operational hydrology report 21, WMO, Geneva, 91 pp., https://library.wmo.int/doc_num.php?explnum_id=1238 (last access: 1 September 2022), 1982.

Sevruk, B.: Point precipitation measurements: why are they not corrected?, in: Water for the future: Proceedings, edited by: Rodda, J. C., IAHS Pr. Inst. of Hydrology, Wallingford, 477–486, https://citeseerx.ist.psu.edu/document?repid=rep1&type=pdf&doi=ed8fec51c8bcdac8f8128cccea655235346ffbe1 (last access: 1 May 2022), 1987.

Sevruk, B. and Chvíla, B.: Error sources of precipitation measurements using electronic weight systems, Atmos. Res., 77, 39–47, https://doi.org/10.1016/j.atmosres.2004.10.026, 2005.

Sevruk, B. and Hamon, W. R.: International Comparison of National Precipitation Gauges with a Reference Pit Gauge, WMO Instrument and Observing Methods Report No. 17, Geneva, https://library.wmo.int/index.php?lvl=notice_display&id=9875 (last access: 1 September 2022), 1984.

Sevruk, B. and Nespor, V.: The Effect of Dimensions and Shape of Precipitation Gauges on the Wind-Induced Error, in: Global Precipitations and Climate Change, edited by: Desbois, M. and Désalmand, F., Springer, Berlin, Heidelberg, 231–246, https://doi.org/10.1007/978-3-642-79268-7_14, 1994.

Sevruk, B., Hertig, A. H., and Spiess, R.: Wind Field Deformation Above Precipitation Gage Orifices, in: IAHS-AGU Symposium on Atmospheric Deposition, edited by: Delleur, J. W. and Miller, J. M., May 1989, Baltimore, Maryland, USA, ISBN 0-947571-86-8, 65–70, 1989.

Shedekar, V. S., King, K. W., Fausey, N. R., Soboyejo, A. B., Harmel, R. D., and Brown, L. C.: Assessment of measurement errors and dynamic calibration methods for three different tipping bucket rain gauges, Atmos. Res., 178–179, 445–458, https://doi.org/10.1016/j.atmosres.2016.04.016, 2016.

Sugiura, K., Yang, D., and Ohata, T.: Systematic error aspects of gauge-measured solid precipitation in the Arctic, Barrow, Alaska, Geophys. Res. Lett., 30, 4, https://doi.org/10.1029/2002GL015547, 2003.

Sugiura, K., Ohata, T., and Yang, D.: Catch Characteristics of Precipitation Gauges in High-Latitude Regions with High Winds, J. Hydrometeorol., 7, 984–994, https://doi.org/10.1175/JHM542.1, 2006.

Tapiador, F. J., Navarro, A., Levizzani, V., García-Ortega, E., Huffman, G. J., Kidd, C., Kucera, P. A., Kummerow, C. D., Masunaga, H., Petersen, W. A., Roca, R., Sánchez, J.-L., Tao, W.-K., and Turk, F. J.: Global precipitation measurements for validating climate models, Atmos. Res., 197, 1–20, https://doi.org/10.1016/j.atmosres.2017.06.021, 2017.

TERENO: Data Discovery Portal, TERENO [data set], https://teodoor.icg.kfa-juelich.de/ddp/index.jsp (last access: 1 September 2022), 2023.

Vaughan, P. J. and Ayars, J. E.: Noise Reduction Methods for Weighing Lysimeters, J. Irrig. Drain Eng., 135, 235–240, https://doi.org/10.1061/(ASCE)0733-9437(2009)135:2(235), 2009.

von Unold, G. and Fank, J.: Modular Design of Field Lysimeters for Specific Application Needs, Water Air Soil Pollut., 8, 233–242, https://doi.org/10.1007/s11267-007-9172-4, 2008.

Vuerich, E., Monesi, C., Lanza, L., Stagi, L., and Lanzinger, E.: WMO Field Intercomparison of Rainfall Intensity Gauges, Instruments and Observing Methods Rep. No. 99, WMO/TD No. 1504, World Meteorological Organisation, https://library.wmo.int/index.php?lvl=notice_display&id=1552 (last access: 1 September 2022), 2009.

Watson, S., Smith, C. D., Lassi, M., and Misfeldt, J.: An Evaluation of the Effectiveness of the Double Alter Wind Shield for Increasing the Catch Efficiency of the Geonor T-200B Precipitation Gauge, CMOS Bulletin SCMO, 36, 168–175, 2008.

Wickham, H.: ggplot2: Elegant graphics for data analysis, in: 2nd Edn., Use R!, Springer, Switzerland, 260 pp., https://doi.org/10.1007/978-0-387-98141-3, 2016.

Winder, P. and Paulson, K. S.: The measurement of rain kinetic energy and rain intensity using an acoustic disdrometer, Meas. Sci. Technol., 23, 15801, https://doi.org/10.1088/0957-0233/23/1/015801, 2012.

WMO: Guide to hydrological practices, in: 6th Edn., World Meteorological Organization, Geneva, 2 pp., https://library.wmo.int/index.php?lvl=notice_display&id=21815 (last access: 1 September 2022), 2008.

WMO: Guide to Meteorological Instruments and Methods of Observation: Volume I – Measurement of Meteorological Variables, WMO, 8, World Meteorological Organization, Geneva, 1177 pp., https://library.wmo.int/index.php?id=12407&lvl=notice_display (last access: 1 September 2022), 2018.

Wolff, M. A., Isaksen, K., Petersen-Øverleir, A., Ødemark, K., Reitan, T., and Brækkan, R.: Derivation of a new continuous adjustment function for correcting wind-induced loss of solid precipitation: results of a Norwegian field study, Hydrol. Earth Syst. Sci., 19, 951–967, https://doi.org/10.5194/hess-19-951-2015, 2015.

Wong, K. and Nitu, R.: CIMO Survey On National Summaries Of Methods And Instruments For Solid Precipitation Measurement At Automatic Weather Stations, Instruments And Observing Methods Report No. 102, WMO, Swizerland, https://library.wmo.int/index.php?lvl=notice_display&id=15528 (last access: 1 September 2022), 2010.

Xiao, H., Meissner, R., Seeger, J., Rupp, H., and Borg, H.: Effect of vegetation type and growth stage on dewfall, determined with high precision weighing lysimeters at a site in northern Germany, J. Hydrol., 377, 43–49, https://doi.org/10.1016/j.jhydrol.2009.08.006, 2009a.

Xiao, H., Meissner, R., Seeger, J., Rupp, H., and Borg, H.: Testing the precision of a weighable gravitation lysimeter, Z. Pflanzenernähr. Bodenk., 172, 194–200, https://doi.org/10.1002/jpln.200800084, 2009b.

Yang, D.: Double Fence Intercomparison Reference (DFIR) vs. Bush Gauge for "true" snowfall measurement, J. Hydrol., 509, 94–100, https://doi.org/10.1016/j.jhydrol.2013.08.052, 2014.

Yang, D., Goodison, B. E., Ishida, S., and Benson, C. S.: Adjustment of daily precipitation data at 10 climate stations in Alaska: Application of World Meteorological Organization intercomparison results, Water Resour. Res., 34, 241–256, https://doi.org/10.1029/97WR02681, 1998.

Yang, D., Goodison, B. E., Metcalfe, J. R., Louie, P., Leavesley, G., Emerson, D., Hanson, C. L., Golubev, V. S., Elomaa, E., Gunther, T., Pangburn, T., Kang, E., and Milkovic, J.: Quantification of precipitation measurement discontinuity induced by wind shields on national gauges, Water Resour. Res., 35, 491–508, https://doi.org/10.1029/1998WR900042, 1999a.

Yang, D., Ishida, S., Goodison, B. E., and Gunther, T.: Bias correction of daily precipitation measurements for Greenland, J. Geophys. Res., 104, 6171–6181, https://doi.org/10.1029/1998JD200110, 1999b.

Yang, D., Kane, D. L., Hinzman, L. D., Goodison, B. E., Metcalfe, J. R., Louie, P. Y. T., Leavesley, G. H., Emerson, D. G., and Hanson, C. L.: An evaluation of the Wyoming Gauge System for snowfall measurement, Water Resour. Res., 36, 2665–2677, https://doi.org/10.1029/2000WR900158, 2000.

Yang, D., Goodison, B., Metcalfe, J., Louie, P., Elomaa, E., Hanson, C., Golubev, V., Gunther, T., Milkovic, J., and Lapin, M.: Compatibility evaluation of national precipitation gage measurements, J. Geophys. Res., 106, 1481–1491, https://doi.org/10.1029/2000JD900612, 2001.

Zacharias, S., Bogena, H., Samaniego, L., Mauder, M., Fuß, R., Pütz, T., Frenzel, M., Schwank, M., Baessler, C., Butterbach-Bahl, K., Bens, O., Borg, E., Brauer, A., Dietrich, P., Hajnsek, I., Helle, G., Kiese, R., Kunstmann, H., Klotz, S., Munch, J. C., Papen, H., Priesack, E., Schmid, H. P., Steinbrecher, R., Rosenbaum, U., Teutsch, G., and Vereecken, H.: A Network of Terrestrial Environmental Observatories in Germany, Vadose Zone J., 10, 955–973, https://doi.org/10.2136/vzj2010.0139, 2011.

Zhang, Q., Wang, S., Yue, P., and Wang, S.: Variation characteristics of non-rainfall water and its contribution to crop water requirements in China's summer monsoon transition zone, J. Hydrol., 578, 124039, https://doi.org/10.1016/j.jhydrol.2019.124039, 2019.